

Probing new physics through entanglement

Rafael Aoude

University of Edinburgh



THE UNIVERSITY
of EDINBURGH

BNL Theory Seminar - 2023

Based on

Quantum SMEFT tomography: top quark pair production at the LHC

RA, Eric Madge, Fabio Maltoni and Luca Mantani

hep-ph/2203.05619

Phys. Rev. D 106 (2022) 5, 055007

Probing new physics through entanglement in diboson productions

RA, Eric Madge, Fabio Maltoni and Luca Mantani

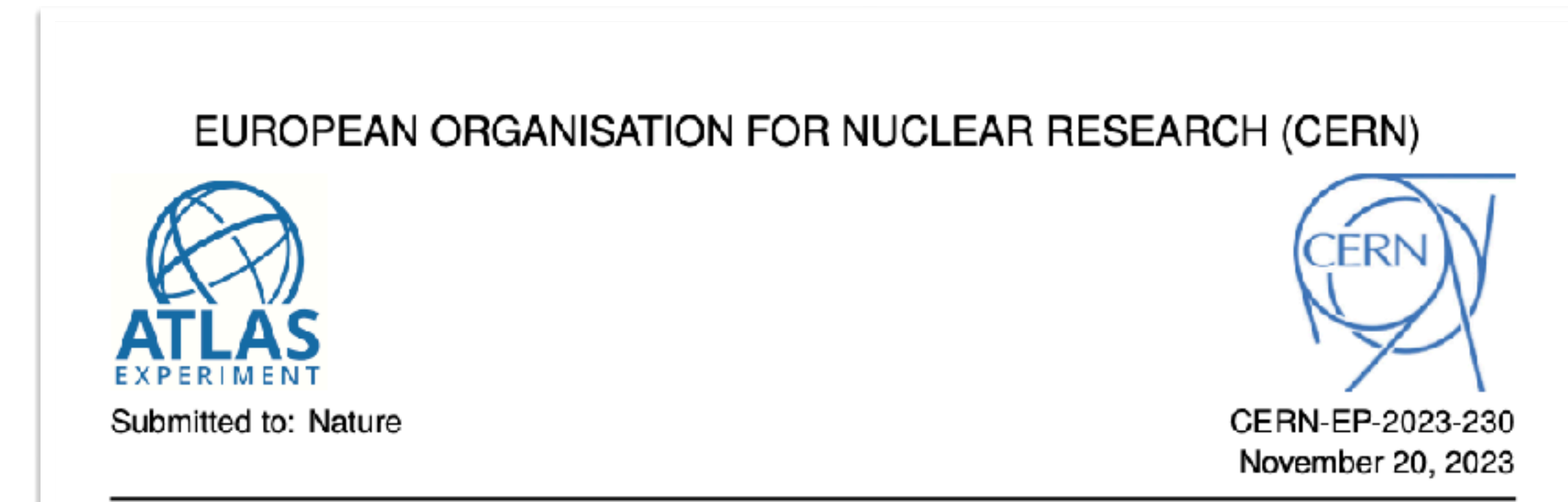
hep-ph/2307.09675

Accepted in JHEP

"I would not call [entanglement] one but rather the characteristic trait of quantum mechanics"

- E. Schrodinger

Fresh new!

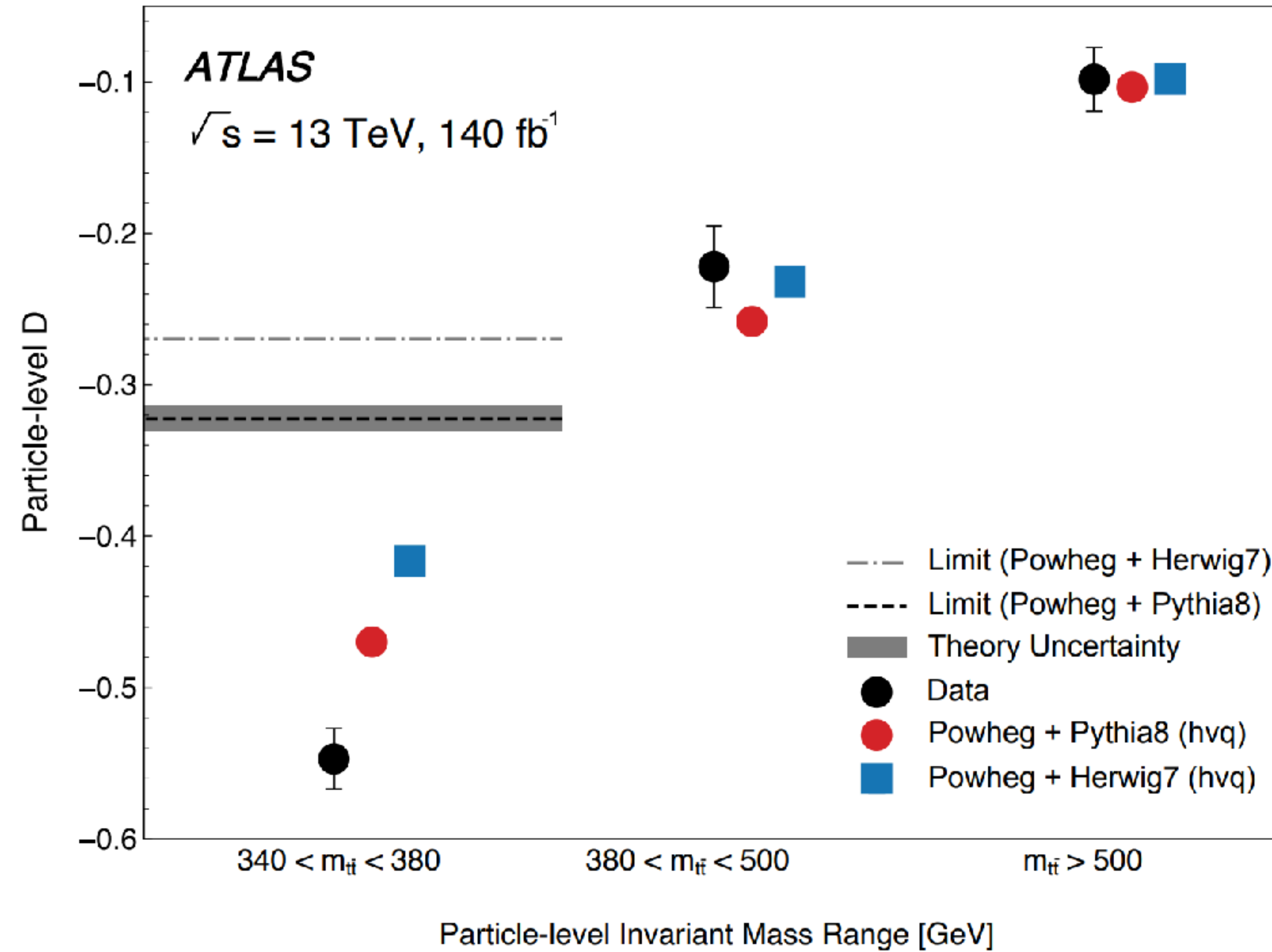


Observation of quantum entanglement in top-quark pairs using the ATLAS detector

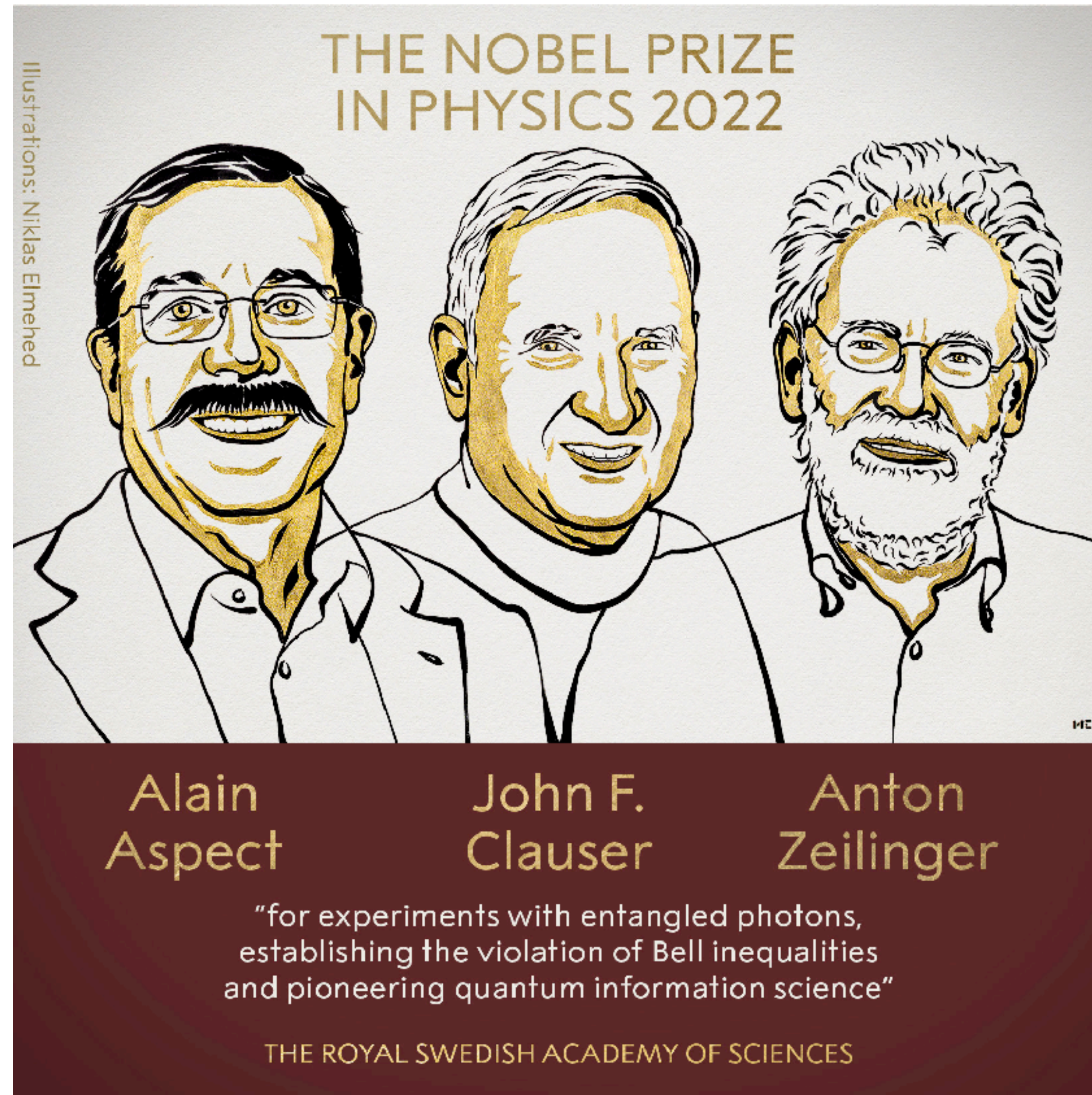
The ATLAS Collaboration

We report the highest-energy observation of entanglement, in top–antitop quark events produced at the Large Hadron Collider, using a proton–proton collision data set with a center-of-mass energy of $\sqrt{s} = 13$ TeV and an integrated luminosity of 140 fb^{-1} recorded with the ATLAS experiment. Spin entanglement is detected from the measurement of a single observable D , inferred from the angle between the charged leptons in their parent top- and antitop-quark rest frames. The observable is measured in a narrow interval around the top–antitop quark production threshold, where the entanglement detection is expected to be significant. It is reported in a fiducial phase space defined with stable particles to minimize the uncertainties that stem from limitations of the Monte Carlo event generators and the parton shower model in modelling top-quark pair production. The entanglement marker is measured to be $D = -0.547 \pm 0.002 \text{ (stat.)} \pm 0.021 \text{ (syst.)}$ for $340 < m_{t\bar{t}} < 380$ GeV. The observed result is more than five standard deviations from a scenario without entanglement and hence constitutes both the first observation of entanglement in a pair of quarks and the highest-energy observation of entanglement to date.

Fresh new!



$D < -1/3 \longleftrightarrow \text{entangled}$



Fastly growing sub-field (since '21)

Bipartite

Top-quark

- [Afik and de Nova, '21]
- [Fabbrichesi, Floreanini, Panizzo, '21]
- [Severi, Degli, Maltoni, Sioli, '21]
- [Aoude, Madge, Maltoni, Mantani, '22]**
- [Afik and de Nova, '22]
- [Aguilar-Saavedra, Casas, '22]
- [Fabbrichesi, Floreanini, Gabrielli, '22]
- [Severi, Vrynidou, '22]
- [Dong, Gonçalves, Kong, Navarro '23]
- [Aguilar-Saavedra, Casas, '23]
- [Han, Low, Wu '23]

...

+ 2 specialised workshops

Foundational tests of Quantum Mechanics at the LHC
Mar 20-23, 2023

Diboson

- [Barr, '21]
- [Barr, Caban, Rembielinski, '22]
- [Aguilar-Saavedra et al '22]
- [Ashby-Pickering, Barr Wierchucka '22]
- [Fabbrichesi et al '23]
- [Aoude, Madge, Maltoni, Mantani, '23]**
- [Aguilar-Saavedra '23]
- [Morales '23]
- [Altomonte, Barr '23]
- [Fabbri, Howarth, Maurin, '23]
- [Bernal, Caban, Rembielinski '23]
- [Bi, Qing-Hong Cao, Cheng, Zhang '23]

...

Tripartite+

- [Bernal, '23]
- [Sakurai, Spannowsky, '23]

+more

$B^0 \rightarrow J/\psi K^*$

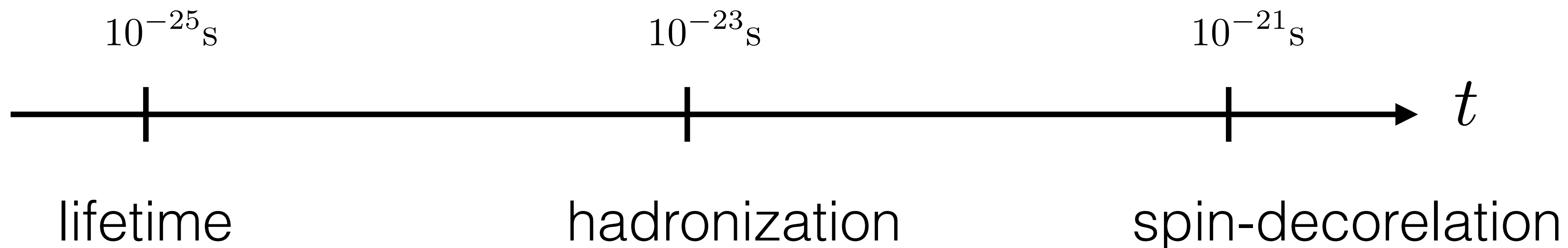
- [Fabbrichesi et al '23]
- ...

Quantum Observables for Collider Physics
Nov 6-10, 2023

Top-pair entanglement



Why top quarks?



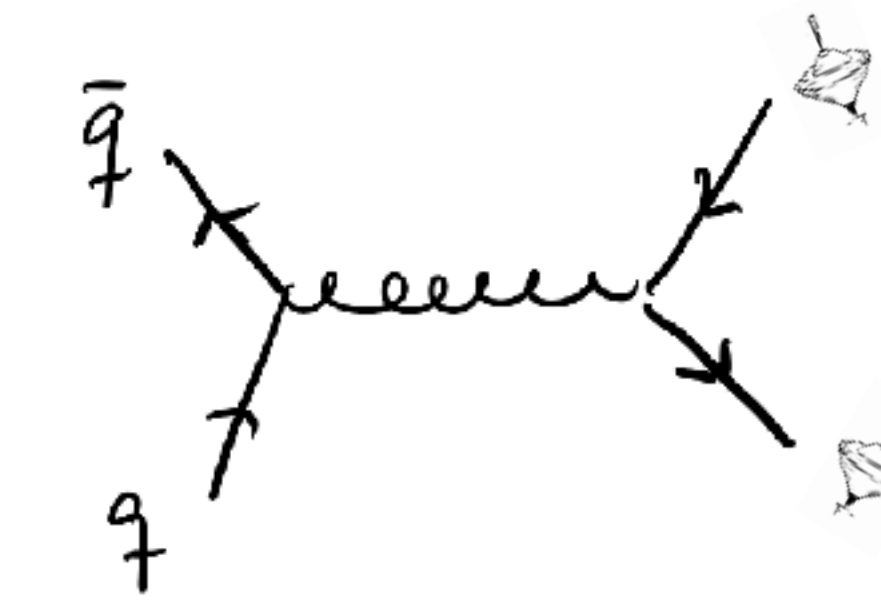
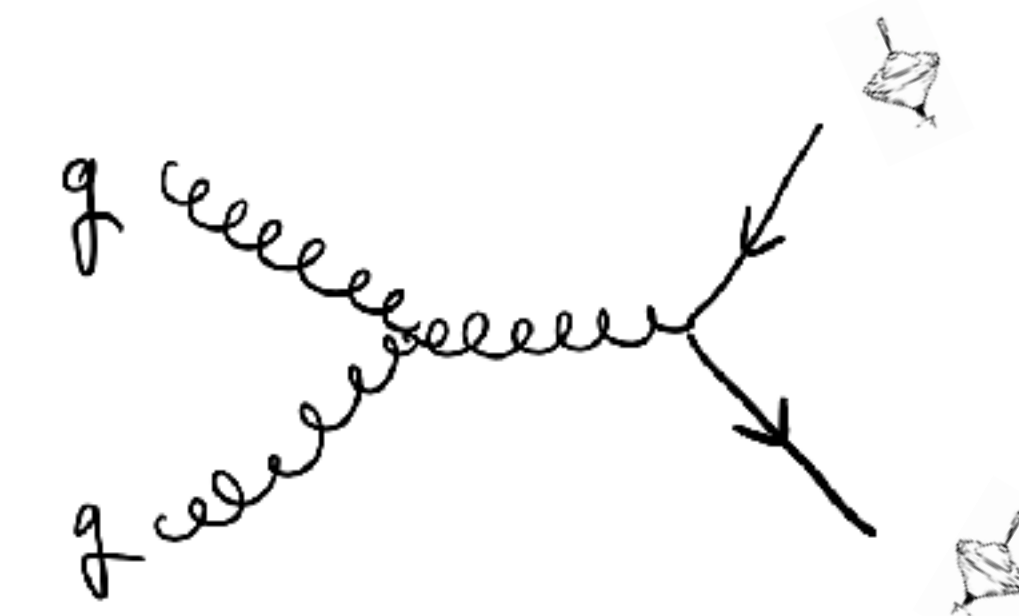
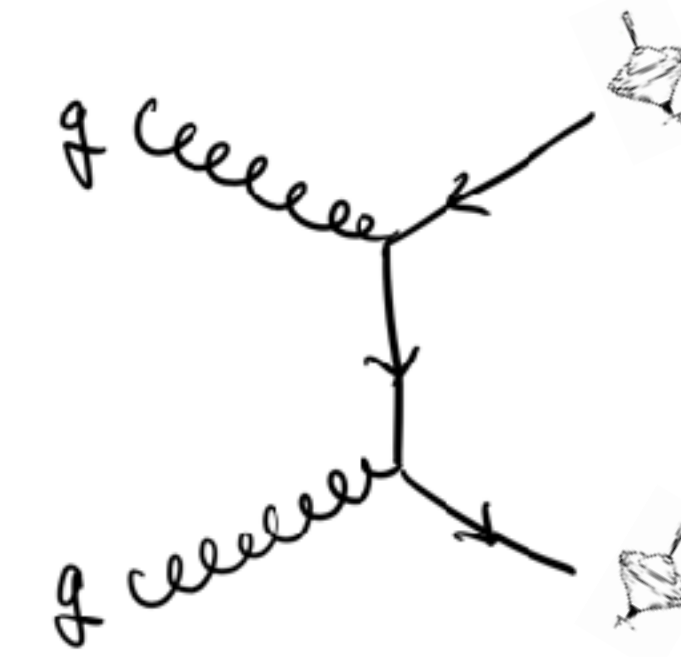
- allows to efficiently reconstruct the spin from decay products
- top spin correlations vastly studied:
 - D0 and CDF at Tevatron and ATLAS and CMS at LHC
- Observation from ATLAS

Entanglement in spin-space

We want the entanglement in the top pair spin



SM:



for instance:

$$\frac{|t(\uparrow)\bar{t}(\uparrow)\rangle + |t(\downarrow)\bar{t}(\downarrow)\rangle}{\sqrt{2}}$$

would be a maximal entangled state

Spin production density matrix

The state-density matrix is obtained from the R-matrix

$$R_{\alpha_1 \alpha_2, \beta_1 \beta_2}^I \equiv \frac{1}{N_a N_b} \sum_{\substack{\text{colors} \\ \text{a,b spins}}} \mathcal{M}_{\alpha_2 \beta_2}^* \mathcal{M}_{\alpha_1 \beta_1}$$

where $\mathcal{M}_{\alpha \beta} \equiv \langle t(k_1, \alpha) \bar{t}(k_2, \beta) | \mathcal{T} | a(p_1) b(p_2) \rangle$

$I = gg, q\bar{q}$

Spin production density matrix

[Afik and de Nova, 21']

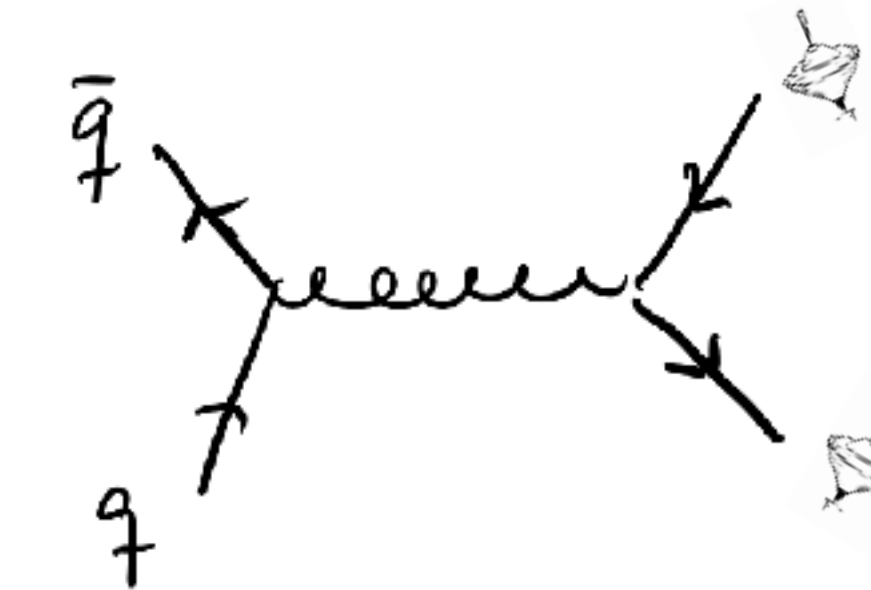
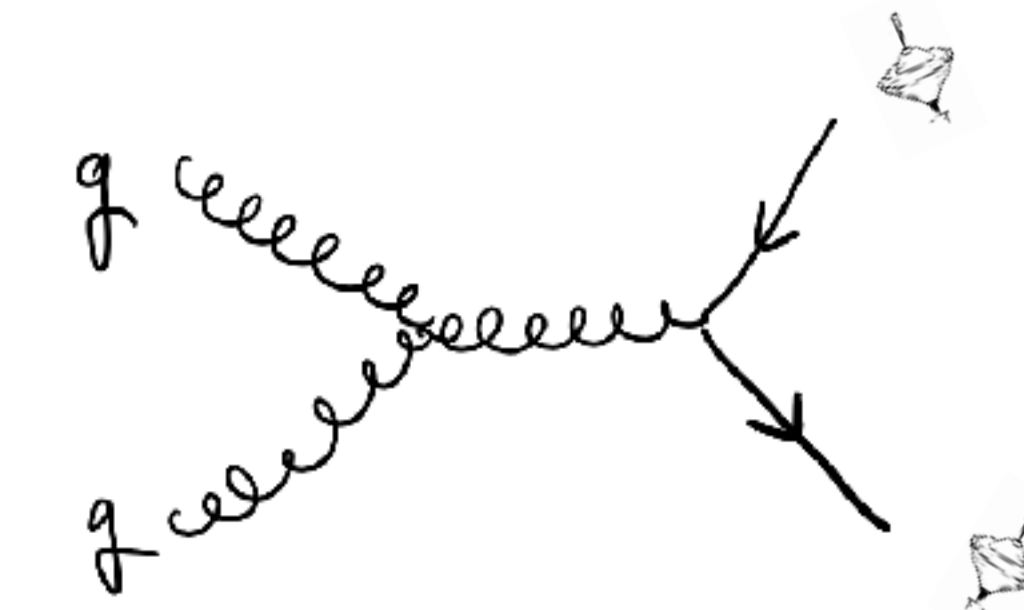
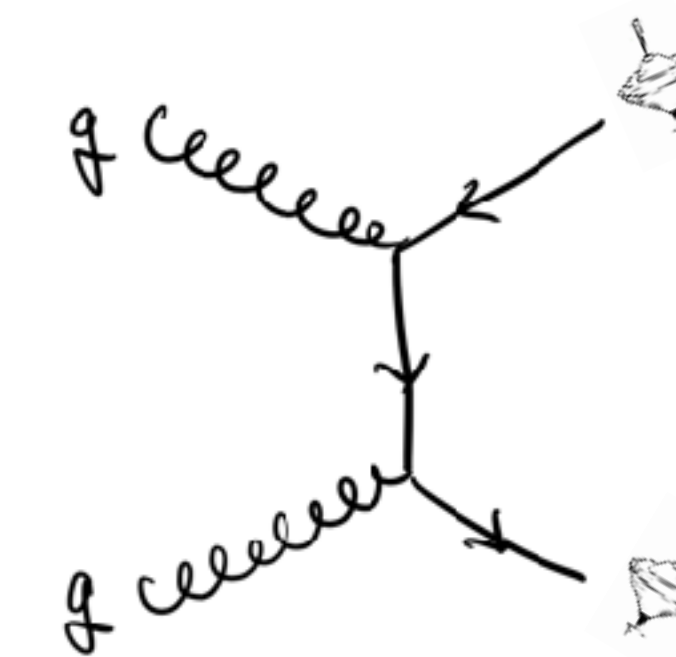
The state-density matrix is obtained from the R-matrix

$$R_{\alpha_1 \alpha_2, \beta_1 \beta_2}^I \equiv \frac{1}{N_a N_b} \sum_{\substack{\text{colors} \\ \text{a,b spins}}} \mathcal{M}_{\alpha_2 \beta_2}^* \mathcal{M}_{\alpha_1 \beta_1}$$

$$I = gg, q\bar{q}$$

$$\text{where } \mathcal{M}_{\alpha\beta} \equiv \langle t(k_1, \alpha) \bar{t}(k_2, \beta) | \mathcal{T} | a(p_1) b(p_2) \rangle$$

SM:



Spin production density matrix

[Afik and de Nova, 21']

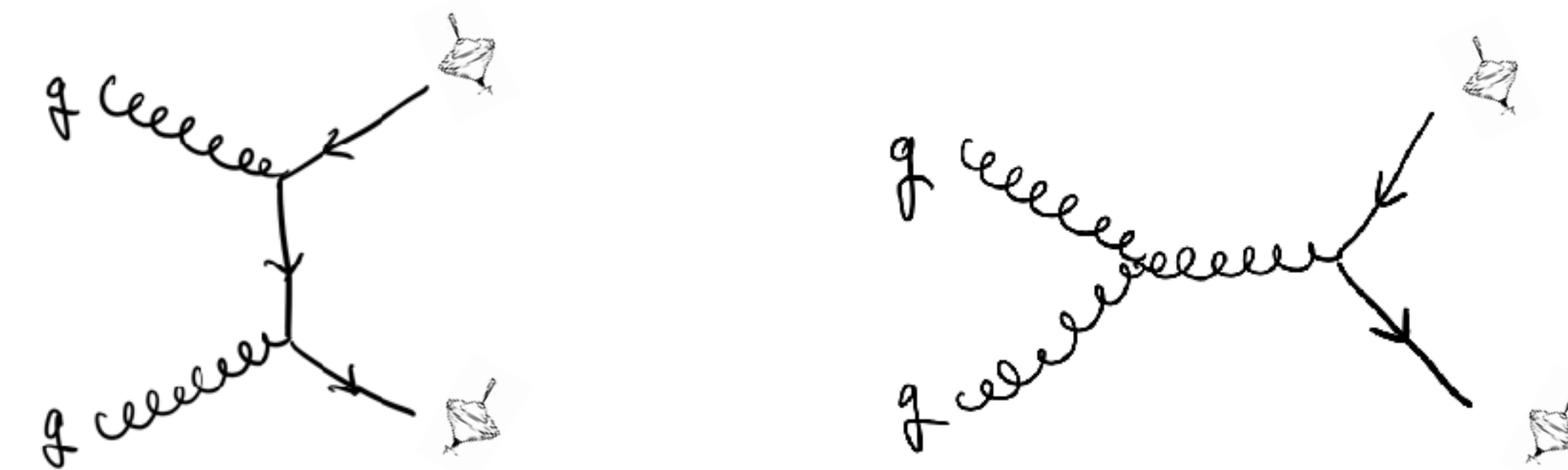
The state-density matrix is obtained from the R-matrix

$$R_{\alpha_1 \alpha_2, \beta_1 \beta_2}^I \equiv \frac{1}{N_a N_b} \sum_{\substack{\text{colors} \\ \text{a,b spins}}} \mathcal{M}_{\alpha_2 \beta_2}^* \mathcal{M}_{\alpha_1 \beta_1}$$

$$I = gg, q\bar{q}$$

$$\text{where } \mathcal{M}_{\alpha\beta} \equiv \langle t(k_1, \alpha) \bar{t}(k_2, \beta) | \mathcal{T} | a(p_1) b(p_2) \rangle$$

SM:



Mixed state of qq and gg initiated channels,
weighted by the luminosity functions

$$R(\hat{s}, \mathbf{k}) = \sum_I L^I(\hat{s}) R^I(\hat{s}, \mathbf{k})$$

Spin production density matrix

[Afik and de Nova, 21']

4x4 matrix in spin-space of the top pair.

Fano decomposition: (spanned by tensor prod. of Pauli and Identity)

$$R = \tilde{A} \mathbf{1}_2 \otimes \mathbf{1}_2 + \tilde{B}_i^+ \sigma^i \otimes \mathbf{1}_2 + \tilde{B}_i^- \mathbf{1}_2 \otimes \sigma^i + \tilde{C}_{ij} \sigma^i \otimes \sigma^j.$$

16-coefficients where the norm

$$\frac{d\sigma}{d\Omega d\hat{s}} = \frac{\alpha_s^2 \beta}{\hat{s}^2} \tilde{A}(\hat{s}, \mathbf{k})$$

Spin production density matrix

[Afik and de Nova, 21']

4x4 matrix in spin-space of the top pair.

Fano decomposition: (spanned by tensor prod. of Pauli and Identity)

$$R = \tilde{A} \mathbf{1}_2 \otimes \mathbf{1}_2 + \tilde{B}_i^+ \sigma^i \otimes \mathbf{1}_2 + \tilde{B}_i^- \mathbf{1}_2 \otimes \sigma^i + \tilde{C}_{ij} \sigma^i \otimes \sigma^j.$$

16-coefficients where the norm

$$\frac{d\sigma}{d\Omega d\hat{s}} = \frac{\alpha_s^2 \beta}{\hat{s}^2} \tilde{A}(\hat{s}, \mathbf{k})$$

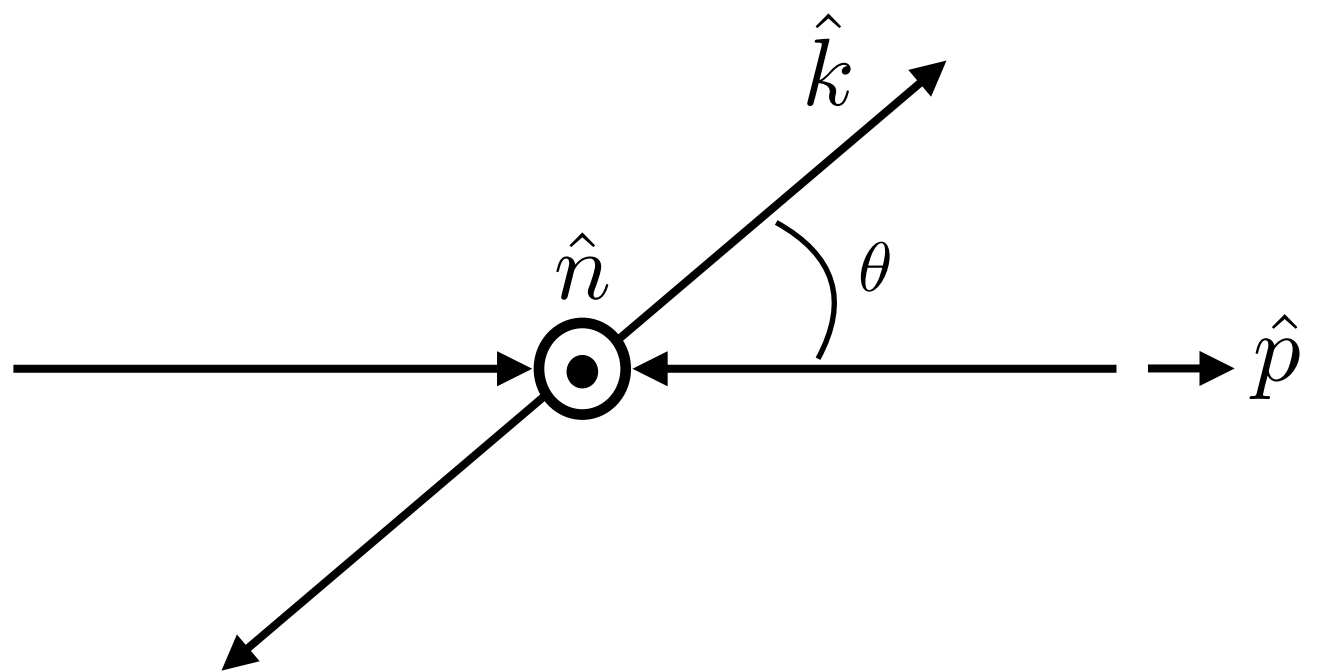
Normalize the state as $\rho = R/\text{tr}(R)$

$$\rho = \frac{\mathbf{1}_2 \otimes \mathbf{1}_2 + B_i^+ \sigma^i \otimes \mathbf{1}_2 + B_i^- \mathbf{1}_2 \otimes \sigma^i + C_{ij} \sigma^i \otimes \sigma^j}{4}.$$

Density matrix and helicity-basis

Helicity basis:

$$\{\mathbf{k}, \mathbf{n}, \mathbf{r}\} : \mathbf{r} = \frac{(\mathbf{p} - z\mathbf{k})}{\sqrt{1 - z^2}}, \quad \mathbf{n} = \mathbf{k} \times \mathbf{r},$$



To expand in this basis, e.g.

$$C_{nn} = \text{tr}[C_{ij} \mathbf{n} \otimes \mathbf{n}]$$

Phase-space parametrized by: $\beta^2 = (1 - 4m_t^2/\hat{s})$ and $z = \cos \theta$

R-matrix coefficients at LO QCD

1. CP invariance $\longrightarrow C_{ij}$ symmetric and $B_i^+ = B_i^-$
2. C_{kn}, C_{rn}, B_n^\pm only generated at one-loop
3. $B_k^\pm B_r^\pm$ require P-odd \longrightarrow vanish for QCD

For gg-initiated SM

$$\begin{aligned}\tilde{A}^{gg,(0)} &= F_{gg}(1 + 2\beta^2(1 - z^2) - \beta^4(z^4 - 2z^2 + 2)), \\ \tilde{C}_{nn}^{gg,(0)} &= -F_{gg}(1 - 2\beta^2 + \beta^4(z^4 - 2z^2 + 2)), \\ \tilde{C}_{kk}^{gg,(0)} &= -F_{gg}(1 - 2z^2(1 - z^2)\beta^2 - (2 - 2z^2 + z^4)\beta^4), \\ \tilde{C}_{rr}^{gg,(0)} &= -F_{gg}(1 - (2 - 2z^2 + z^4)\beta^2(2 - \beta^2)), \\ \tilde{C}_{rk}^{gg,(0)} &= F_{gg} 2z (1 - z^2)^{3/2} \beta^2 \sqrt{1 - \beta^2},\end{aligned}$$

$$F_{gg} = \frac{7 + 9\beta^2 z^2}{192(1 - \beta^2 z^2)^2}$$

Entanglement in bipartite systems

Given a bipartite system $\mathcal{H}_{ab} = \mathcal{H}_a \otimes \mathcal{H}_b$

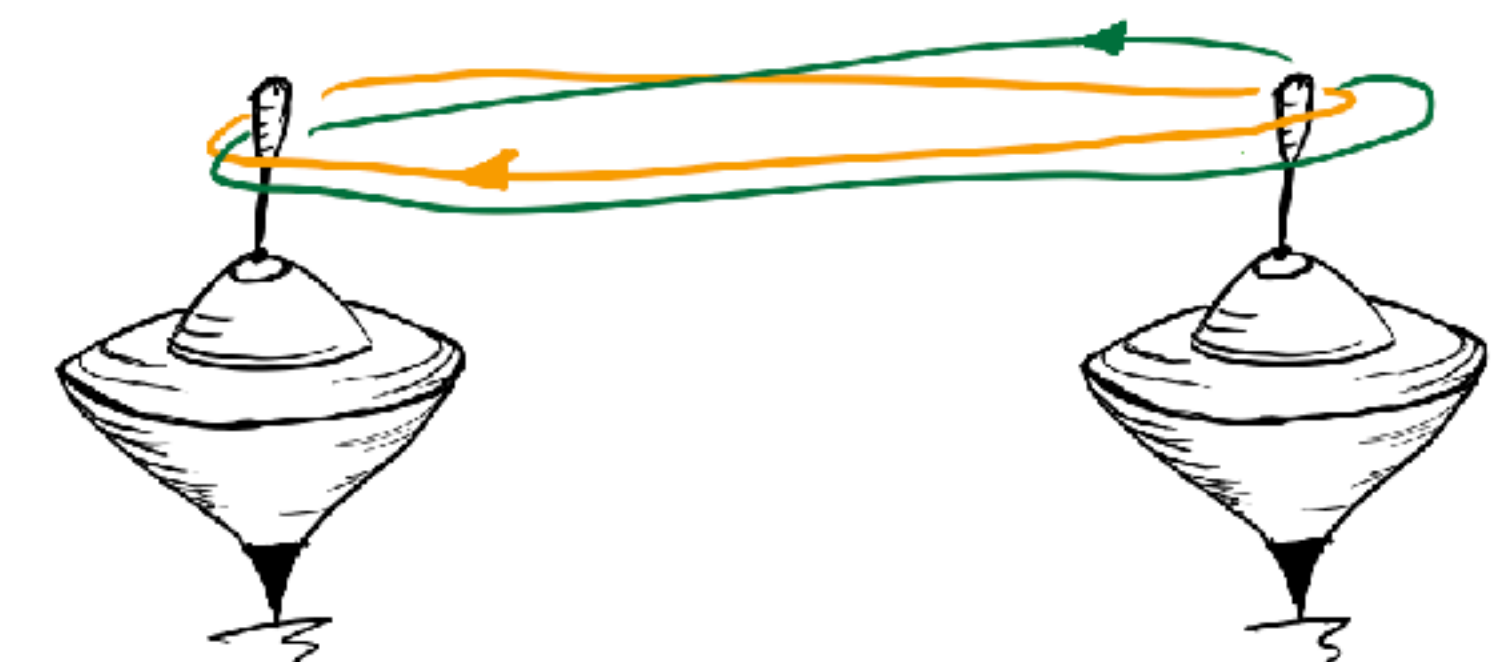
Can you write $|\Psi_{ab}\rangle = |\Psi_a\rangle \otimes |\Psi_b\rangle$?

No? Then it is entangled.

Or more generally as product (mixed states): $\rho_{ab} = \sum_k p_k \rho_a^k \otimes \rho_b^k$

Maximally entangled states (e.g Bell states):

$$|\Phi^\pm\rangle = \frac{|\uparrow\uparrow\rangle \pm |\downarrow\downarrow\rangle}{\sqrt{2}} \quad \text{or} \quad |\Psi^\pm\rangle = \frac{|\uparrow\downarrow\rangle \pm |\downarrow\uparrow\rangle}{\sqrt{2}}$$



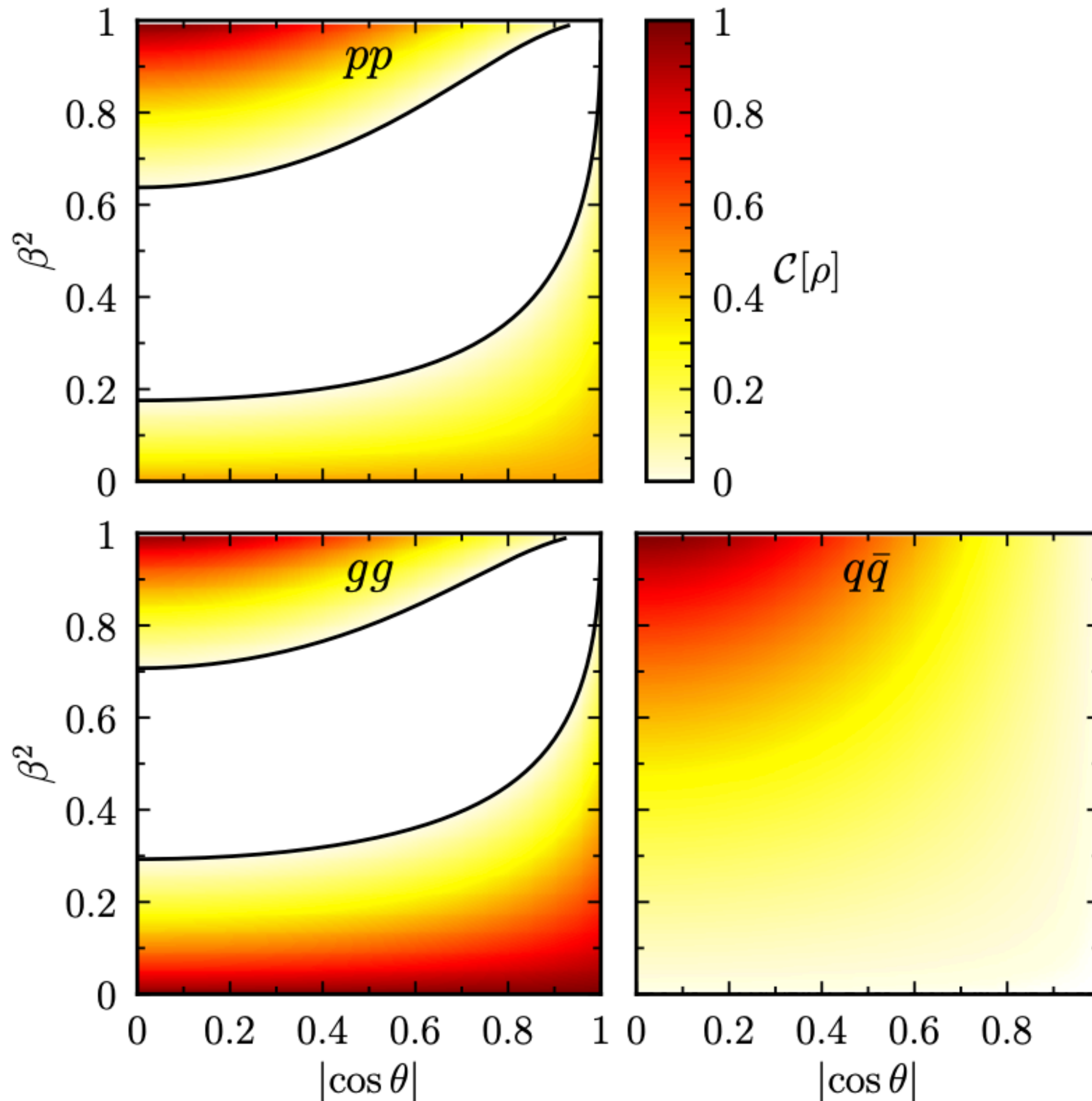
Entanglement in bipartite systems

Entanglement measures are more useful:

- Peres-Horodecki Criterion: $\Delta \equiv -C_{nn} + |C_{kk} + C_{rr}| - 1 > 0$
(in the helicity-basis) (entangled)
- Concurrence: $C[\rho] = \max(\Delta/2, 0)$
 $C[\rho] = 1$ (maximally entangled)

What's the story for the SM?

[Afik and de Nova, 21']



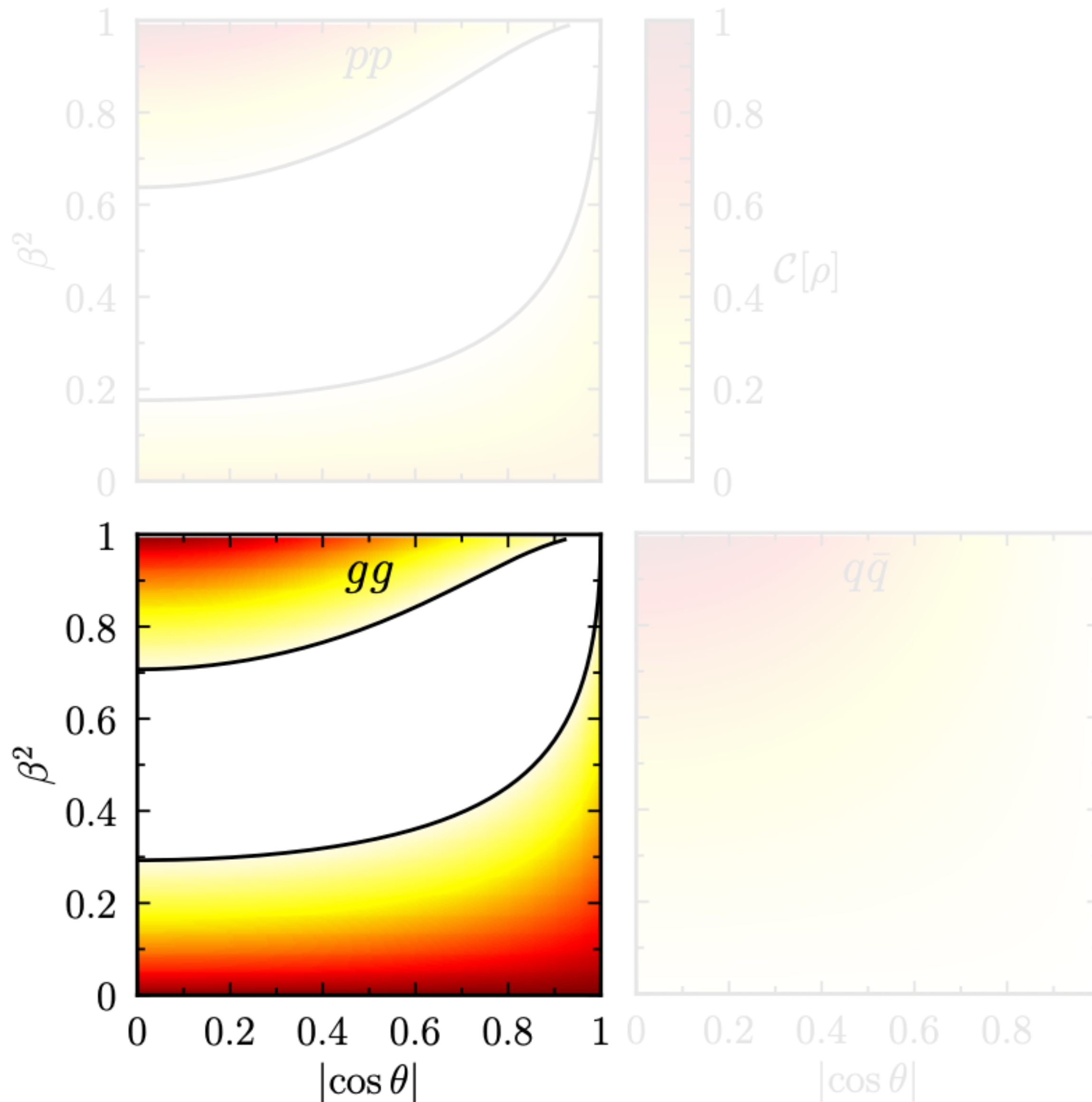
White regions: zero-entanglement

Maximal entanglement points/regions

- At threshold: $\beta^2 = 0, \forall \theta$
- high-E: $\beta^2 \rightarrow 1, \cos \theta = 0$

What's the story for the SM?

[Afik and de Nova, 21']



Maximal entanglement points/regions

- At threshold: $\beta^2 = 0, \forall \theta$

(singlet)

$$\rho_{gg}^{\text{SM}}(0, z) = |\Psi^-\rangle_n \langle \Psi^-|_n$$

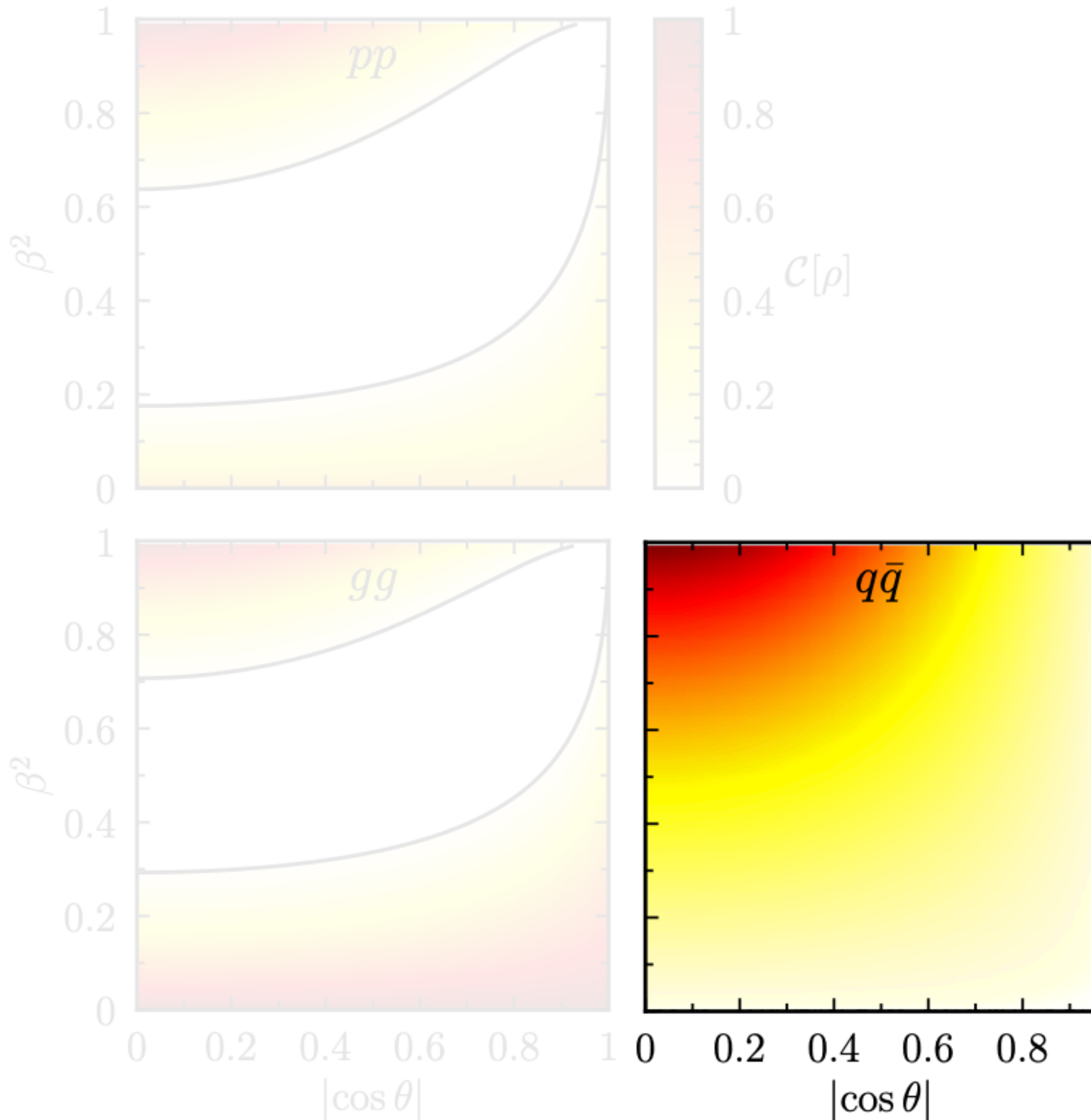
- high-E: $\beta^2 \rightarrow 1, \cos \theta = 0$

(triplet)

$$\rho_{gg}^{\text{SM}}(1, 0) = |\Psi^+\rangle_n \langle \Psi^+|_n$$

What's the story for the SM?

[Afik and de Nova, 21']



Maximal entanglement points/regions

- At threshold: $\beta^2 = 0, \forall \theta$

mixed but separable

- high-E: $\beta^2 \rightarrow 1, \cos \theta = 0$

(triplet: same as gg)

$$\rho_{q\bar{q}}^{\text{SM}}(1, 0) = |\Psi^+\rangle_{\mathbf{n}} \langle \Psi^+|_{\mathbf{n}}.$$

Tomography and reconstruction of the state

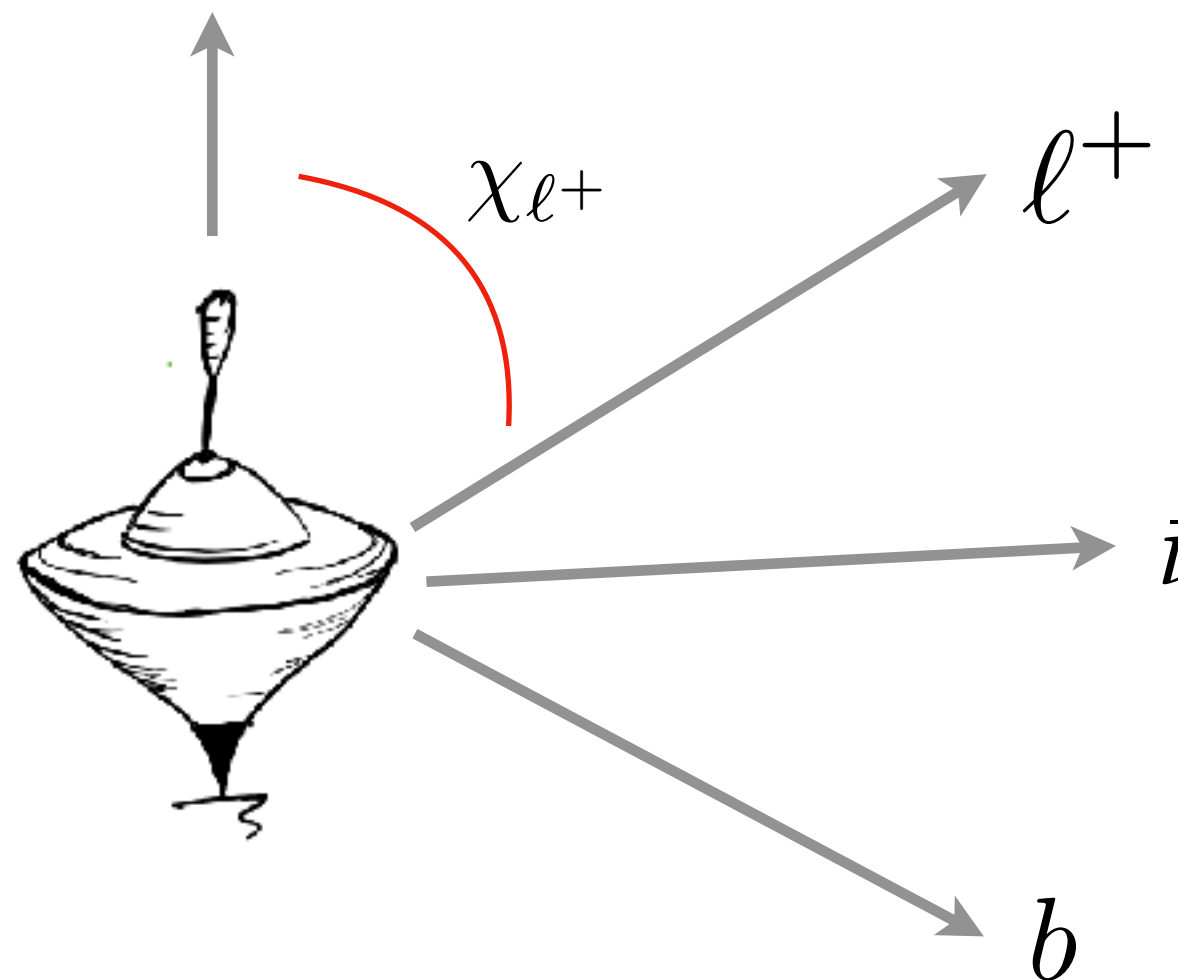
[Mahlon, Parke 10']

[Baumgart, Tweede 12']

[Afik and de Nova, 21']

$\Gamma_t \sim 1\text{GeV}$ top quickly decays \longrightarrow spin-info to decay products

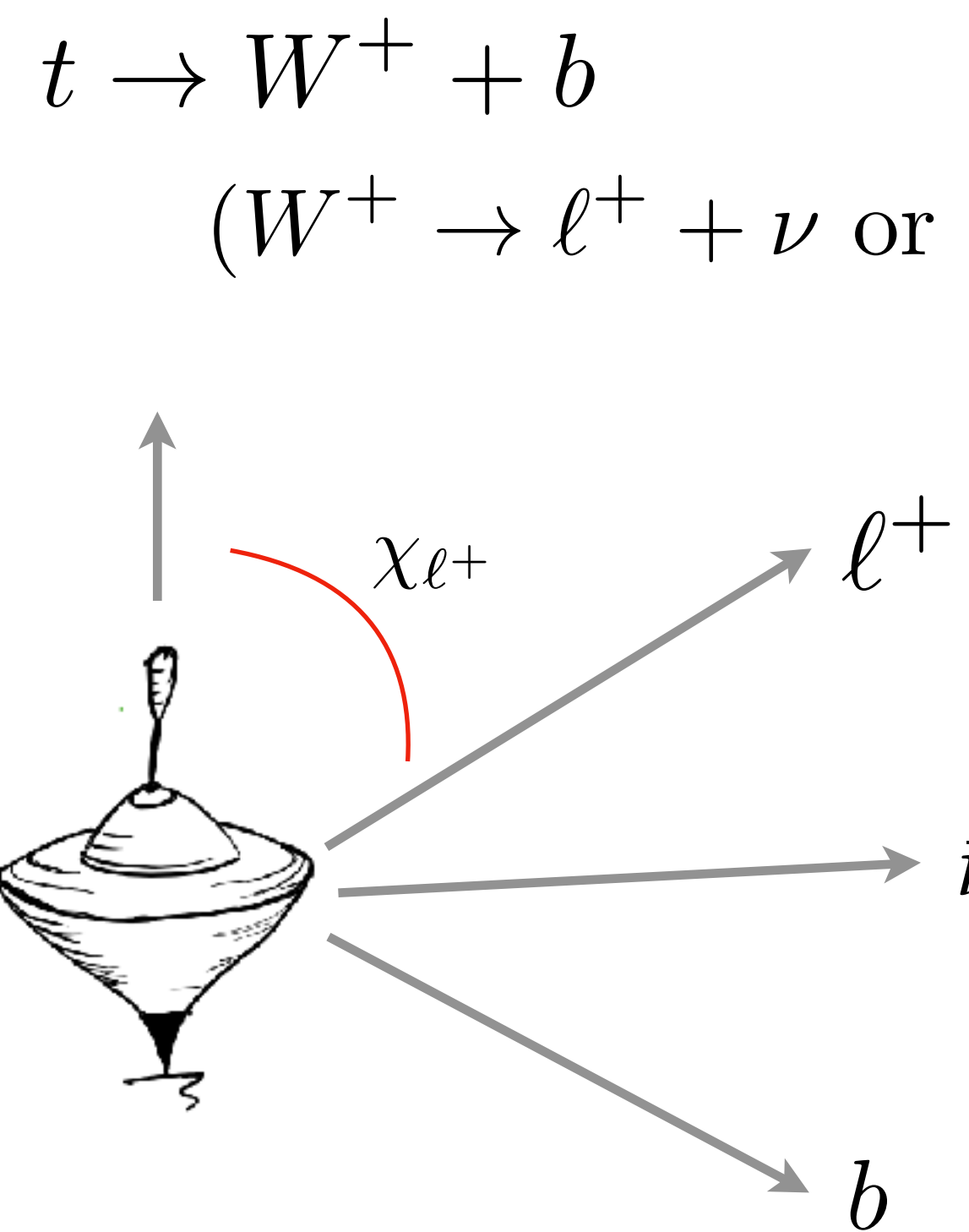
$$t \rightarrow W^+ + b$$
$$(W^+ \rightarrow \ell^+ + \nu \text{ or } \bar{d} + u)$$



Tomography and reconstruction of the state

[Mahlon, Parke 10']
[Baumgart, Tweede 12']
[Afik and de Nova, 21']

$\Gamma_t \sim 1\text{GeV}$ top quickly decays \longrightarrow spin-info to decay products



$$\frac{1}{\Gamma_t} \frac{d\Gamma}{d \cos \chi_i}$$

$$= (1 + \alpha_i \cos \chi_i)/2 \quad \alpha_i = \begin{cases} +1.0 & \ell^+ \text{ or } \bar{d}\text{-quark} \\ -0.31 & \bar{\nu} \text{ or } u\text{-quark} \\ -0.41 & b\text{-quark} \end{cases}$$

χ_i angle between i-th particle and top spin (top rest frame)

Tomography and reconstruction of the state

[Mahlon, Parke 10']

[Baumgart, Tweede 12']

[Afik and de Nova, 21']

$\Gamma_t \sim 1\text{GeV}$ top quickly decays \longrightarrow spin-info to decay products

$$t \rightarrow W^+ + b$$
$$(W^+ \rightarrow \ell^+ + \nu \text{ or } \bar{d} + u) \quad \frac{1}{\Gamma_t} \frac{d\Gamma}{d \cos \chi_i} = (1 + \alpha_i \cos \chi_i)/2 \quad \alpha_i = \begin{cases} +1.0 & \ell^+ \text{ or } \bar{d}\text{-quark} \\ -0.31 & \bar{\nu} \text{ or } u\text{-quark} \\ -0.41 & b\text{-quark} \end{cases}$$

When both top/antitop have lepton in the decay, the angles **(fixed beam basis)**

$$\frac{1}{\sigma} \frac{d\sigma}{d\Omega_+ d\Omega_-} = \frac{1 + \mathbf{B}^+ \cdot \hat{\mathbf{q}}_+ - \mathbf{B}^- \cdot \hat{\mathbf{q}}_- - \hat{\mathbf{q}}_+ \cdot \mathbf{C} \cdot \hat{\mathbf{q}}_-}{(4\pi)^2}$$

$\hat{\mathbf{q}}_{\pm}$ lepton (antilepton) directions in the parent top (antitop) rest frame

[CMS, PRD 100, 072002]

Experimental detection

[Baumgart, Tweede 12']

[Afik and de Nova, 21']

However, there is a direct experimental signature

[Aguilar-Saavedra, Casas, '22]

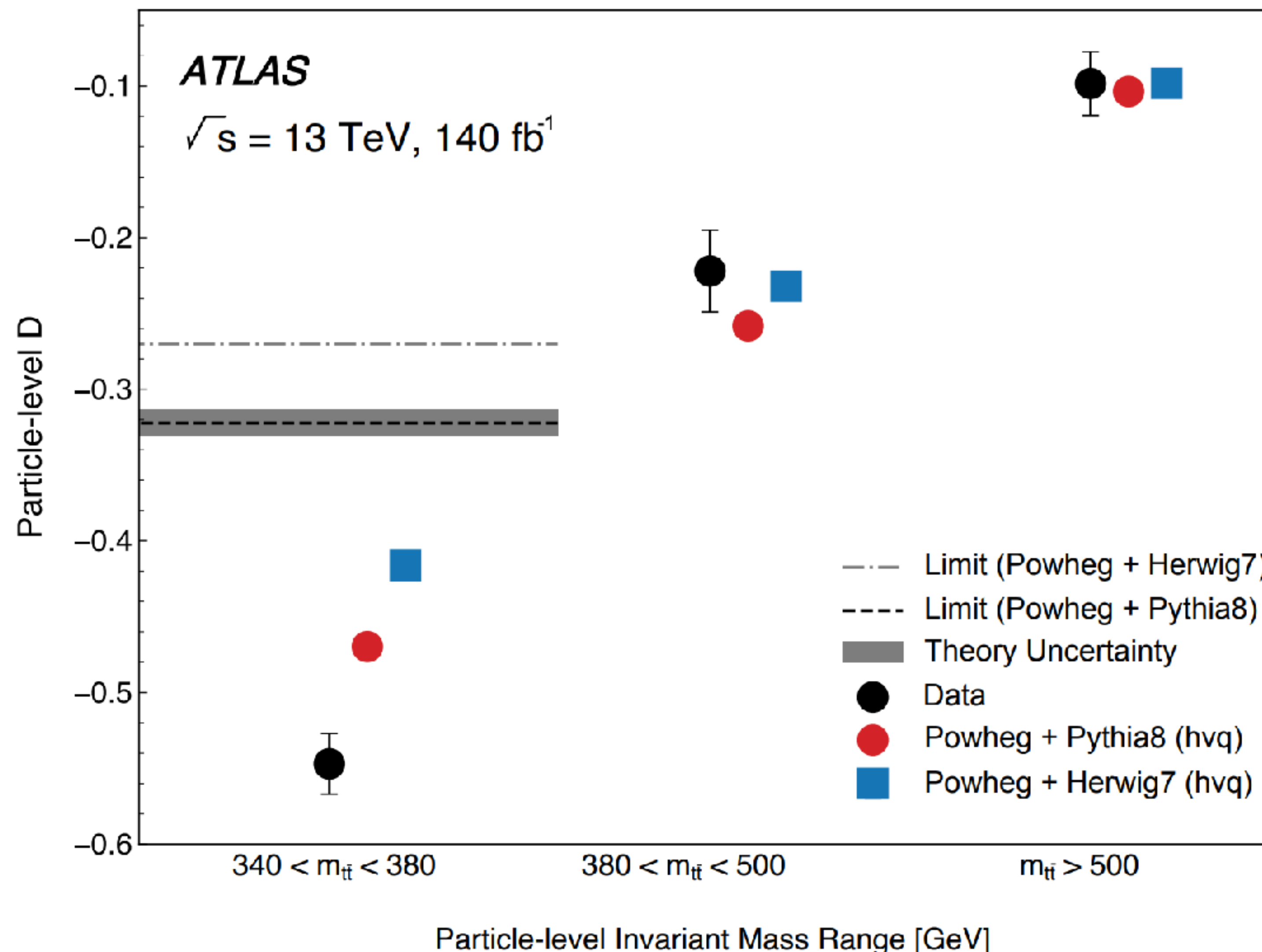
$$D = \frac{\text{tr}[\mathbf{C}]}{3} \longrightarrow \frac{1}{\sigma} \frac{d\sigma}{d \cos \varphi} = \frac{1}{2} (1 - D \cos \varphi)$$

φ angle between leptons in each parent direction rest frames

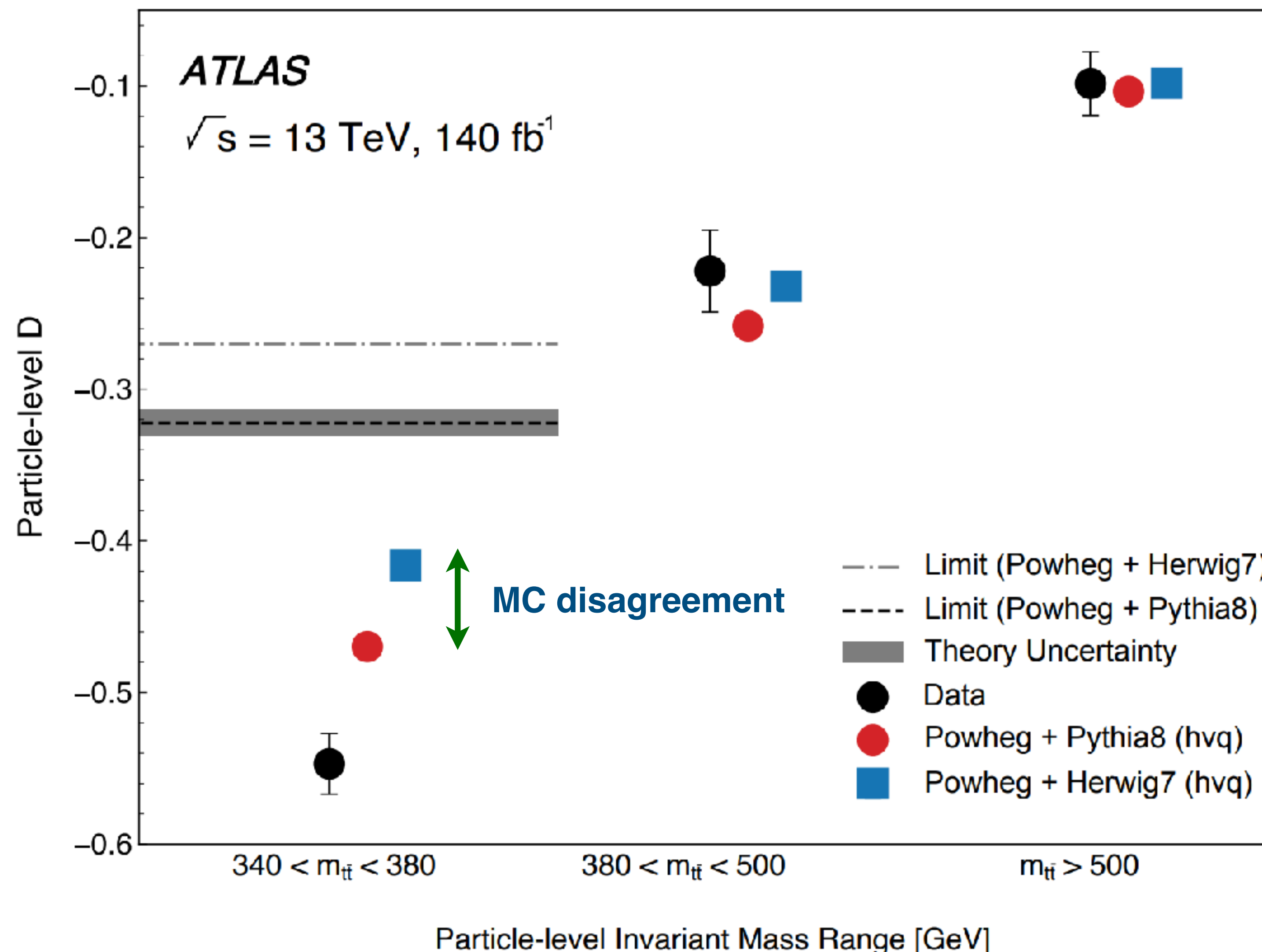
$$C[\rho] = \max(1 - 3D, 0)/2 \longrightarrow \text{entangled if } D < -1/3$$

* things are actually more subtle due to mass window constraints

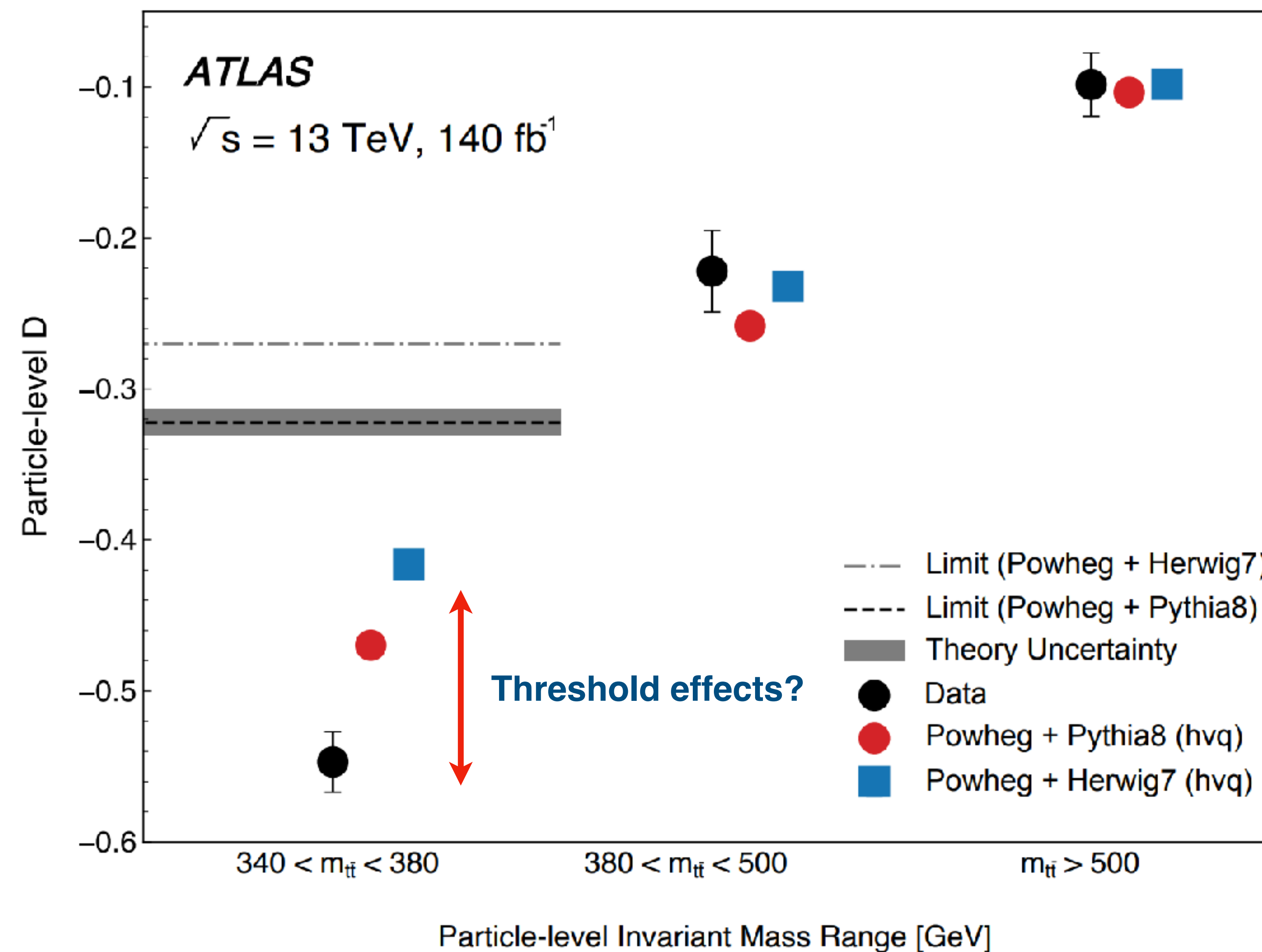
Experimental detection



Experimental detection



Experimental detection



Too early for any fit or claim in this region!!

SM particles

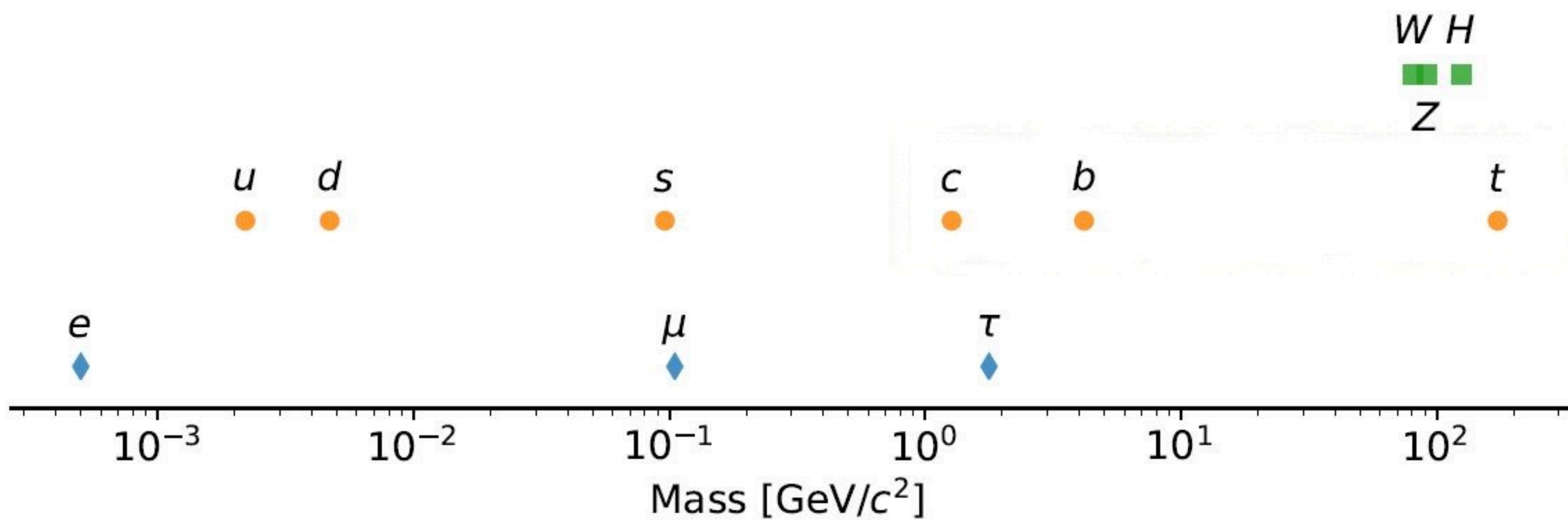


[Fig from CMS collaboration]

BSM particles?

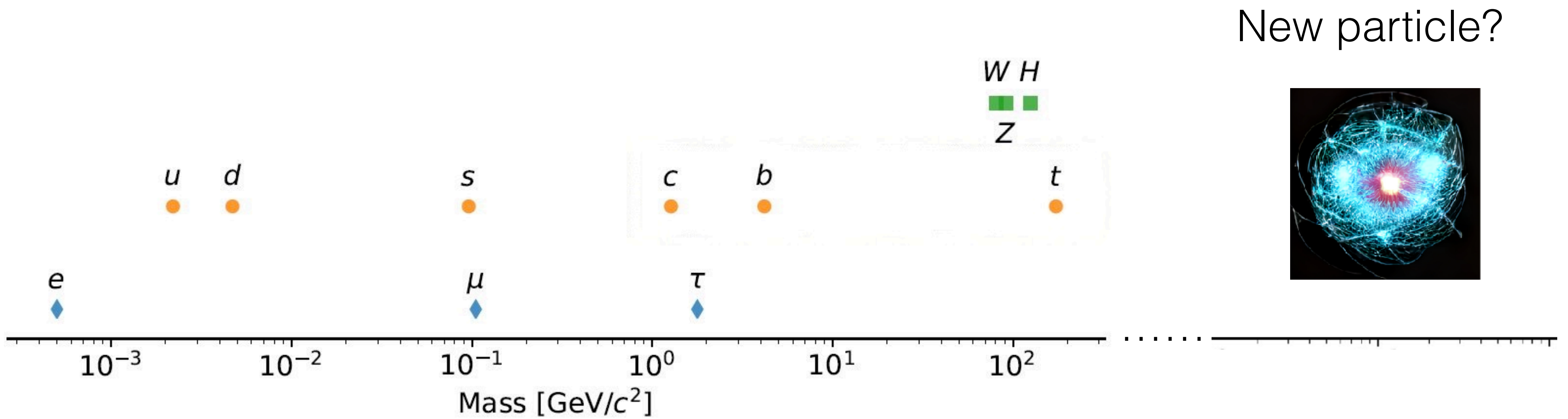
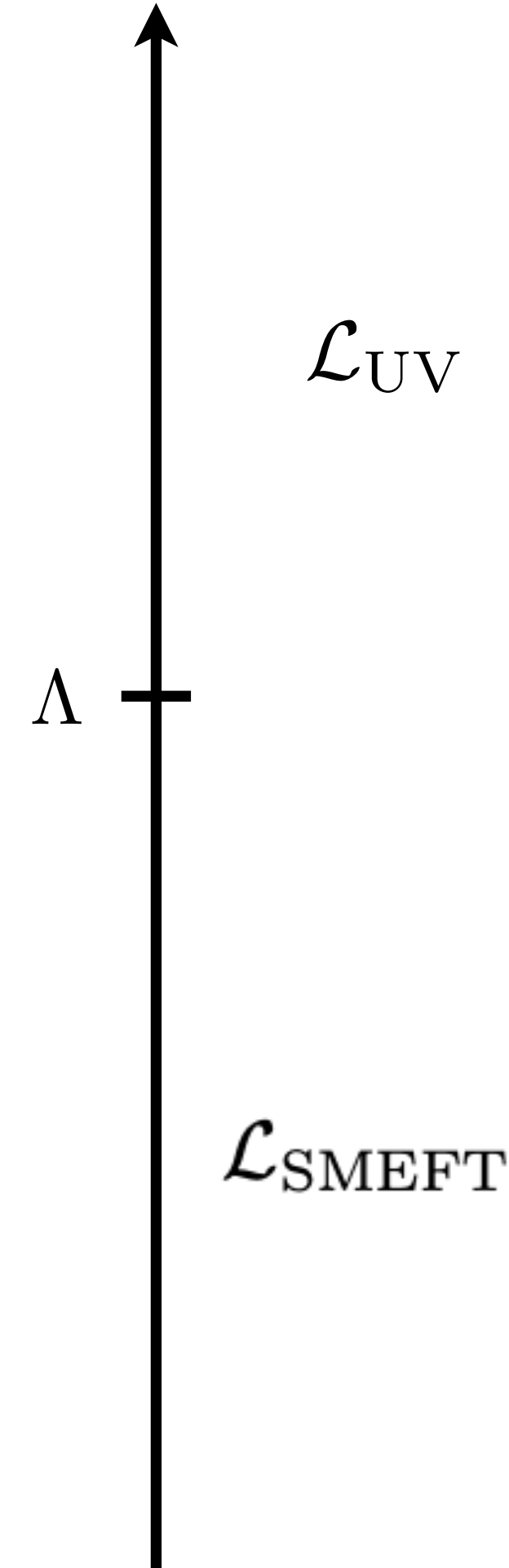


[Fig from CMS collaboration]

SMEFT



$$\mathcal{L}_{\text{SMEFT}} = \mathcal{L}_{\text{SM}} + \frac{1}{\Lambda^2} \sum_i c_i \mathcal{O}_i$$

LO-QCD in ttbar prod.

$$\mathcal{O}_G = g_s f^{ABC} G_{\nu}^{A,\mu} G_{\rho}^{B,\nu} G_{\mu}^{C,\rho}$$

$$\mathcal{O}_{\varphi G} = \left(\varphi^\dagger \varphi - \frac{v^2}{2} \right) G_A^{\mu\nu} G_{\mu\nu}^A$$

$$\mathcal{O}_{tG} = g_s (\bar{Q} \sigma^{\mu\nu} T^A t) \tilde{\varphi} G_{\mu\nu}^A + \text{h.c.}$$

[Grzadkowski, Iskrzynski, Misiak, Rosiek, 10']

[Aguilar-Saavedra et. al, 18']

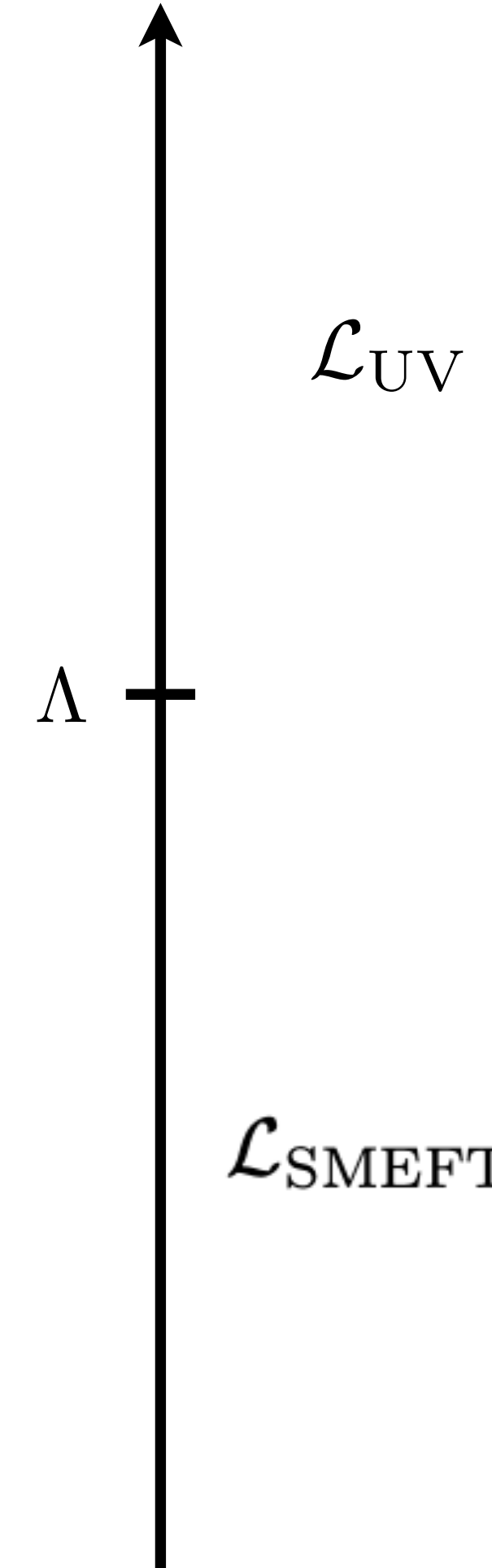
[SMEFTatNLO: Degrande et. al, 20']

+4F operators

$$\mathcal{O}_{Qq}^{(8,1)}, \mathcal{O}_{Qq}^{(8,3)}, \mathcal{O}_{tu}^{(8)}, \mathcal{O}_{td}^{(8)}, \mathcal{O}_{Qu}^{(8)}, \mathcal{O}_{Qd}^{(8)}, \mathcal{O}_{tq}^{(8)}$$

SMEFT

$$\mathcal{L}_{\text{SMEFT}} = \mathcal{L}_{\text{SM}} + \frac{1}{\Lambda^2} \sum_i c_i \mathcal{O}_i$$



LO-QCD in ttbar prod.

$$\mathcal{O}_G = g_s f^{ABC} G_\nu^{A,\mu} G_\rho^{B,\nu} G_\mu^{C,\rho}$$

$$\mathcal{O}_{\varphi G} = \left(\varphi^\dagger \varphi - \frac{v^2}{2} \right) G_A^{\mu\nu} G_{\mu\nu}^A$$

$$\mathcal{O}_{tG} = g_s (\bar{Q} \sigma^{\mu\nu} T^A t) \tilde{\varphi} G_{\mu\nu}^A + \text{h.c.}$$

[Grzadkowski, Iskrzynski, Misiak, Rosiek, 10']

[Aguilar-Saavedra et. al, 18']

[SMEFTatNLO: Degrande et. al, 20']

+4F operators

$$\mathcal{O}_{Qq}^{(8,1)}, \mathcal{O}_{Qq}^{(8,3)}, \mathcal{O}_{tu}^{(8)}, \mathcal{O}_{td}^{(8)}, \mathcal{O}_{Qu}^{(8)}, \mathcal{O}_{Qd}^{(8)}, \mathcal{O}_{tq}^{(8)}$$

Maximal points are affected by SMEFT?

Can SMEFT induce new regions?

SMEFT

Back to the R-matrix... $R_{\alpha_1 \alpha_2, \beta_1 \beta_2}^I \equiv \frac{1}{N_a N_b} \sum_{\substack{\text{colors} \\ a, b \text{ spins}}} \mathcal{M}_{\alpha_2 \beta_2}^* \mathcal{M}_{\alpha_1 \beta_1}$

With dim-six contributions:

$$\mathcal{M}_{\alpha\beta} = \mathcal{M}_{\alpha\beta}^{\text{SM}} + \frac{1}{\Lambda^2} \mathcal{M}_{\alpha\beta}^{(\text{d6})} \quad \longrightarrow \quad \rho = \frac{R^{\text{SM}} + R^{\text{EFT}}}{\text{tr}(R^{\text{SM}}) + \text{tr}(R^{\text{EFT}})}$$

The Fano coefficients $X = X^{(0)} + \frac{1}{\Lambda^2} X^{(1)} + \frac{1}{\Lambda^4} X^{(2)}$ where

$$X = \tilde{A}, \tilde{C}_{ij} \text{ and } \tilde{B}_i^\pm$$

$\mathcal{O}(\Lambda^{-4})$ from dim-6 sq.

SMEFT

Back to the R-matrix... $R_{\alpha_1 \alpha_2, \beta_1 \beta_2}^I \equiv \frac{1}{N_a N_b} \sum_{\substack{\text{colors} \\ a, b \text{ spins}}} \mathcal{M}_{\alpha_2 \beta_2}^* \mathcal{M}_{\alpha_1 \beta_1}$

With dim-six contributions:

$$\mathcal{M}_{\alpha\beta} = \mathcal{M}_{\alpha\beta}^{\text{SM}} + \frac{1}{\Lambda^2} \mathcal{M}_{\alpha\beta}^{(\text{d6})} \quad \longrightarrow \quad \rho = \frac{R^{\text{SM}} + R^{\text{EFT}}}{\text{tr}(R^{\text{SM}}) + \text{tr}(R^{\text{EFT}})}$$

At $\mathcal{O}(\Lambda^{-2})$

$$\tilde{C}_{nn}^{gg,(1)} = \frac{g_s^2}{\Lambda^2} \frac{1}{1 - \beta^2 z^2} \left[\frac{-7g_s^2 v m_t}{12\sqrt{2}} c_{tG} - \frac{\beta^2 m_t^4}{4m_t^2 - (1 - \beta^2)m_h^2} c_{\varphi G} + \frac{9g_s^2 \beta^2 m_t^2 z^2}{8} c_G \right]$$

SMEFT entanglement: gg-initiated

[Aoude, Madge,
Maltoni, Mantani, 22']

only $\mathcal{O}_{tG}, \mathcal{O}_G, \mathcal{O}_{\varphi G}$ contributes

$$\rho = \frac{R^{\text{SM}} + R^{\text{EFT}}}{\text{tr}(R^{\text{SM}}) + \text{tr}(R^{\text{EFT}})}$$

gg-initiated at threshold $\beta^2 = 0$

- linear interference exactly cancel, maximally entangled state unchanged
- quadratics vanish for $\mathcal{O}_{\varphi G}$ and decreases for $\mathcal{O}_{tG}, \mathcal{O}_G$

gg-initiated at high-E: $\beta^2 \rightarrow 1$: EFT not valid but $m_t^2 \ll \hat{s} \ll \Lambda^2$

- linear interference: sign dependent
- quadratics always decreases

SMEFT entanglement: qq-initiated

[Aoude, Madge,
Maltoni, Mantani, 22']

only \mathcal{O}_{tG} and 4F contributes

$$\rho = \frac{R^{\text{SM}} + R^{\text{EFT}}}{\text{tr}(R^{\text{SM}}) + \text{tr}(R^{\text{EFT}})}$$

qq-initiated at threshold $\beta^2 = 0$

- no contributions for linear and quad

qq-initiated at high-E: $m_t^2 \ll \hat{s} \ll \Lambda^2$

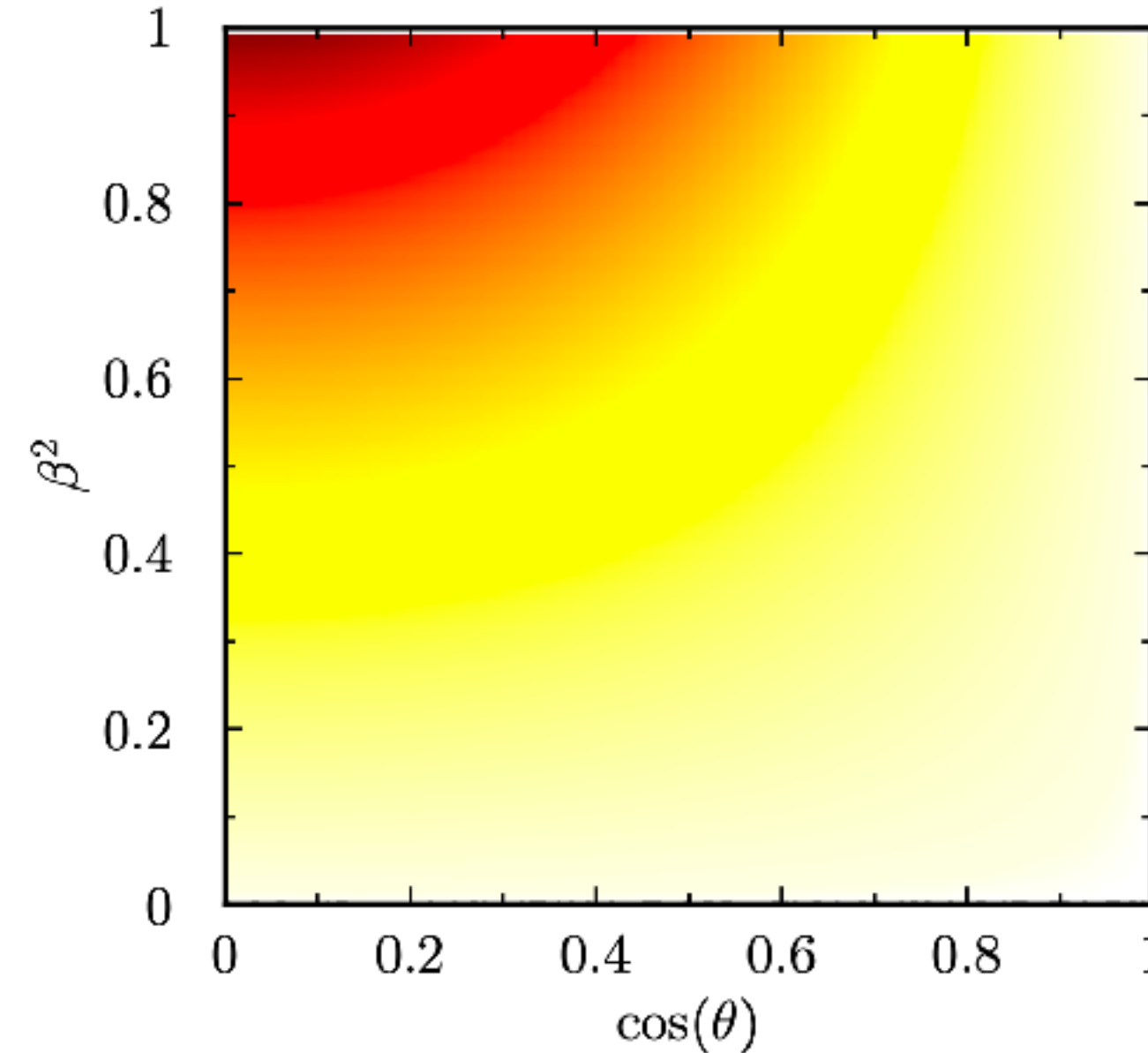
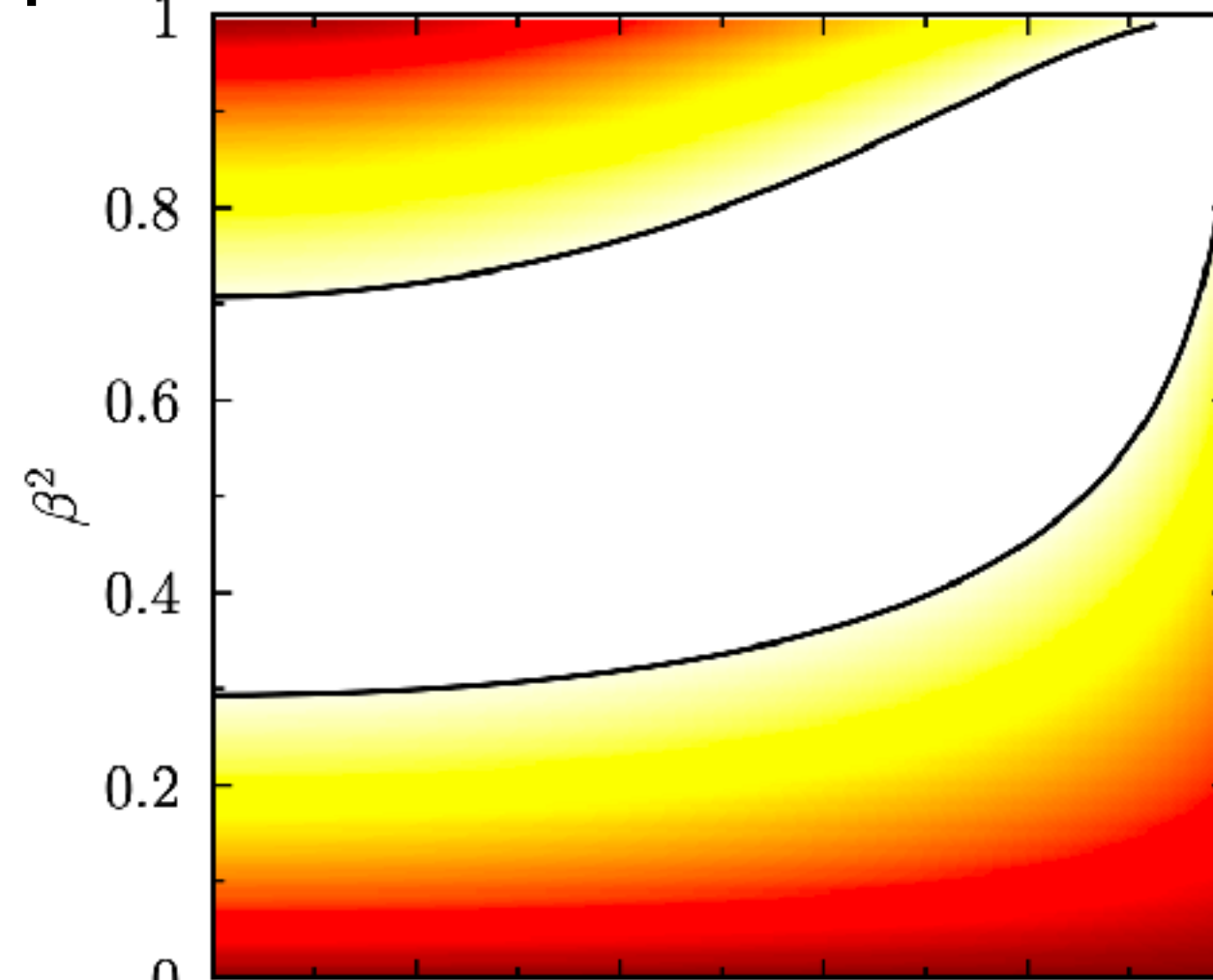
- sign dependent for linear and quadratics always decreases

everything gets more involved for pp

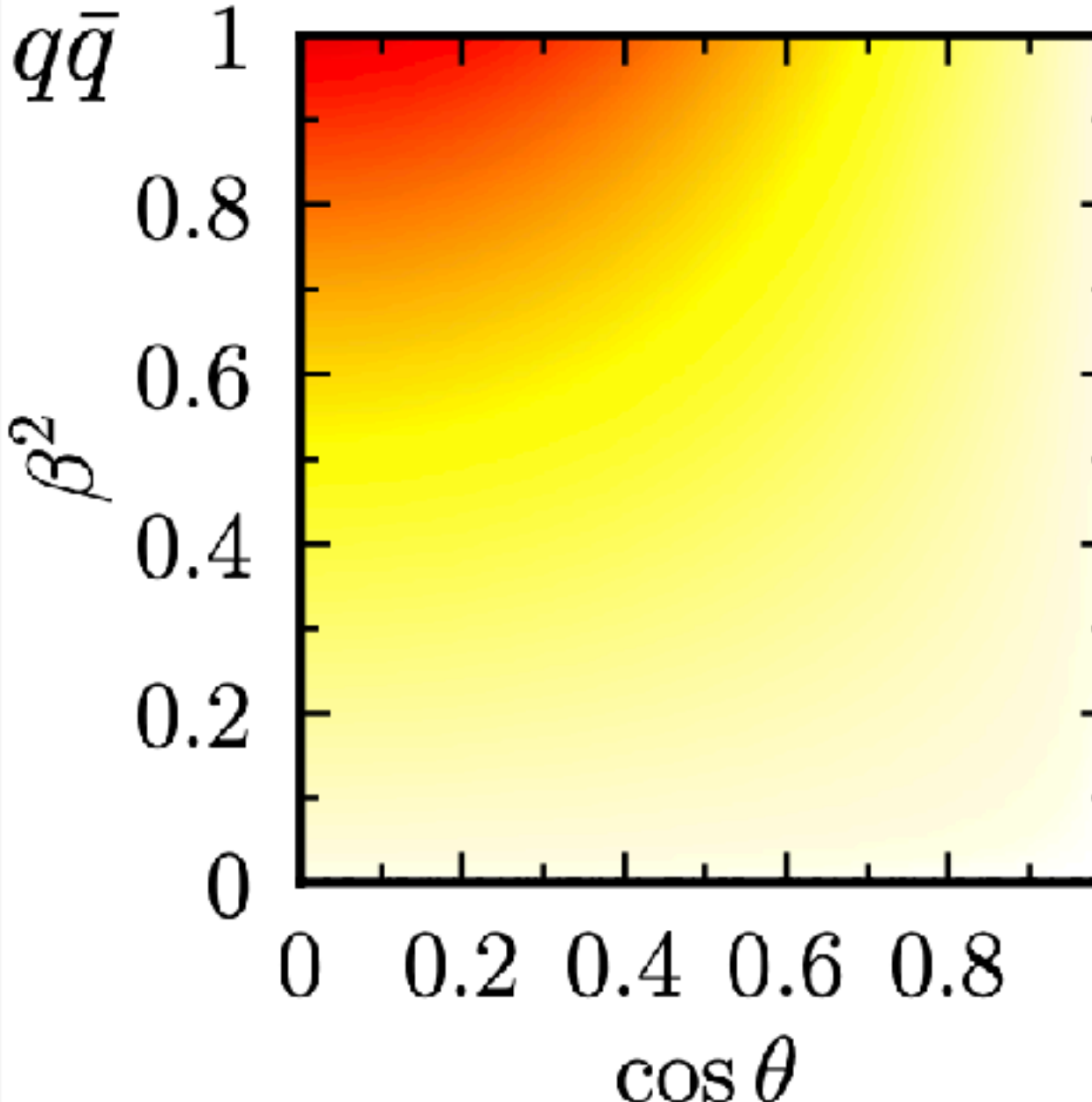
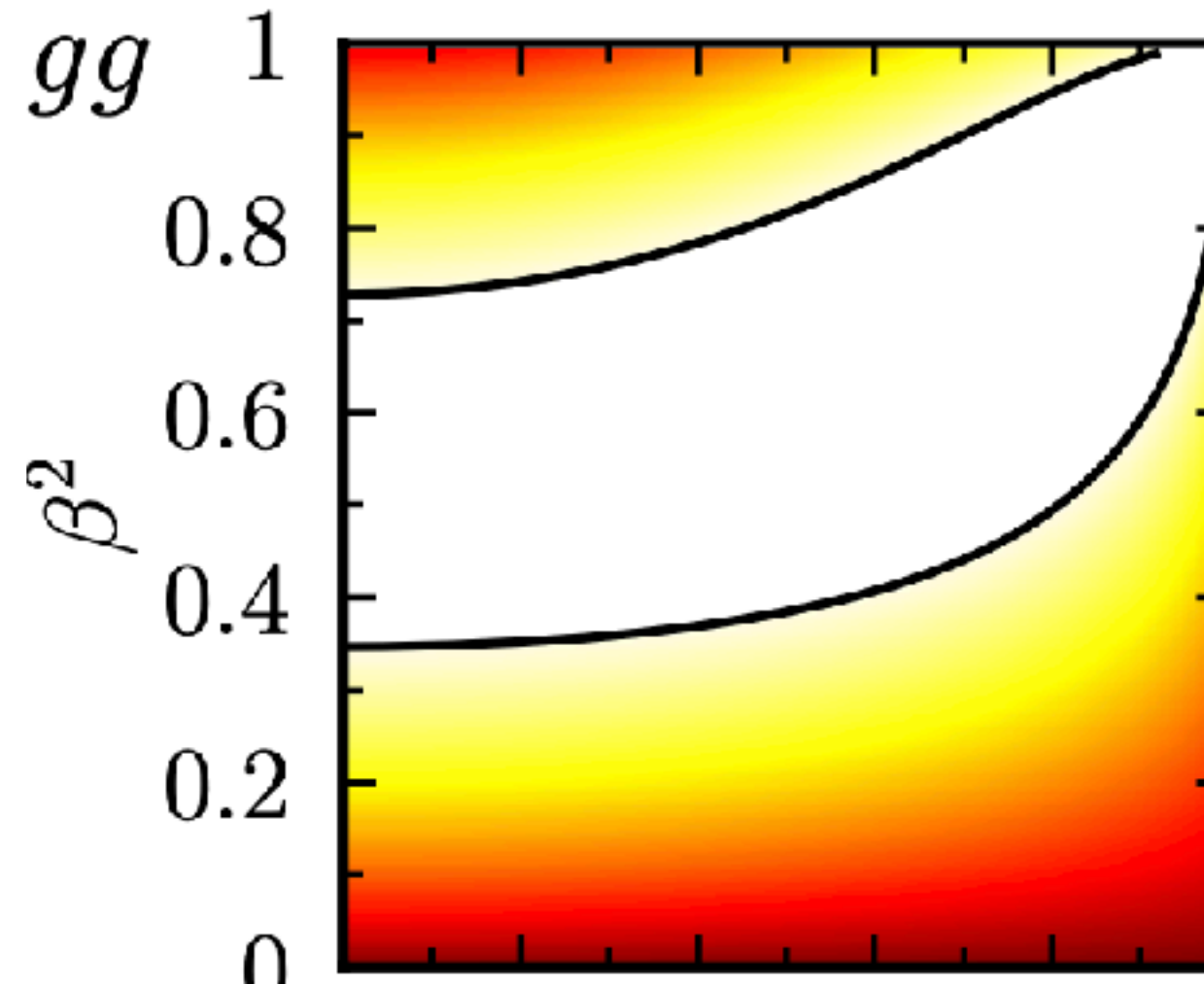
SMEFT entanglement

$$\mathcal{O}_{tG} = g_s(\bar{Q}\sigma^{\mu\nu}T^A t)\tilde{\varphi}G_{\mu\nu}^A + \text{h.c.}$$

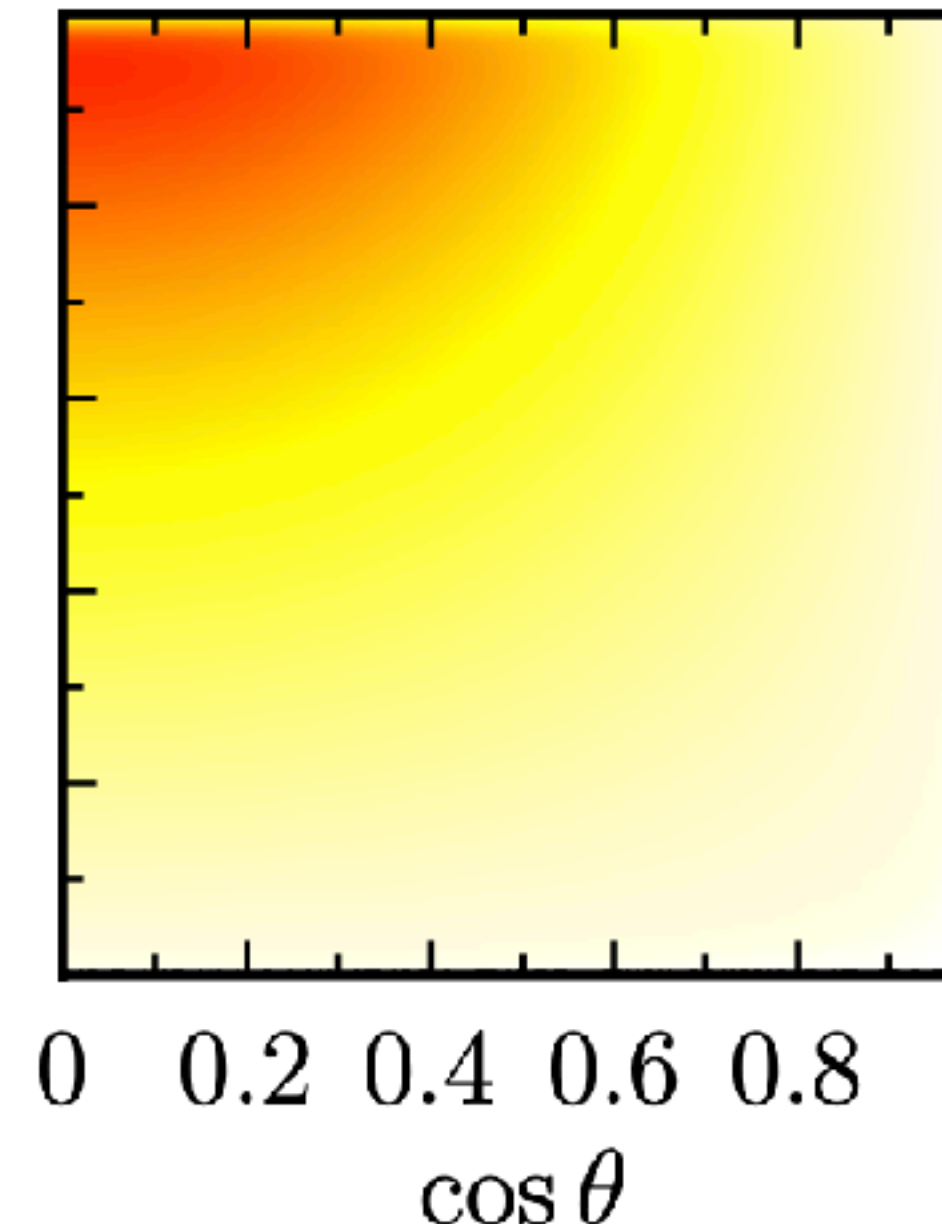
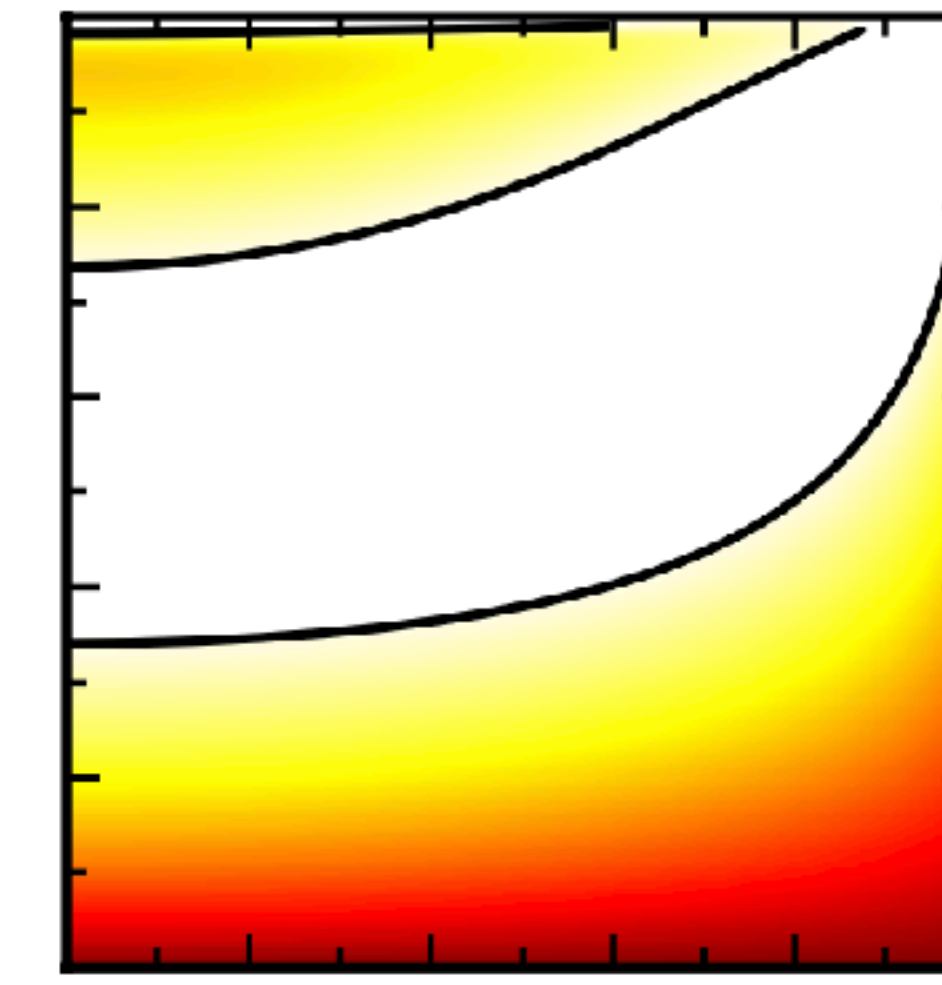
SM



linear



quad

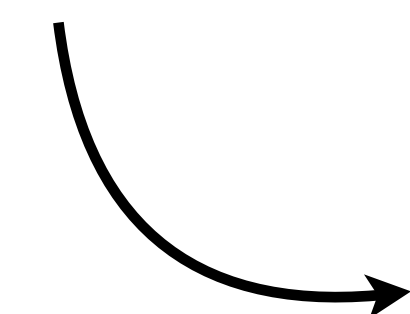


SMEFT entanglement marker

$$\rho = \frac{R^{\text{SM}} + R^{\text{EFT}}}{\text{tr}(R^{\text{SM}}) + \text{tr}(R^{\text{EFT}})}$$

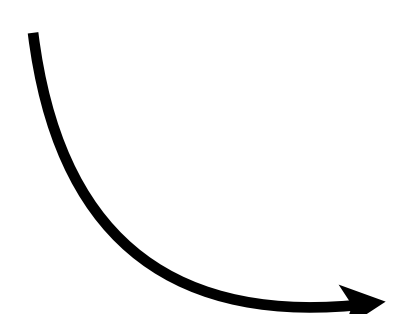
Δ_0 calculated with SM R's

$$\Delta_1 \equiv \Delta - \Delta_0$$



calculated with SMEFT R's up to $\mathcal{O}(\Lambda^{-2})$

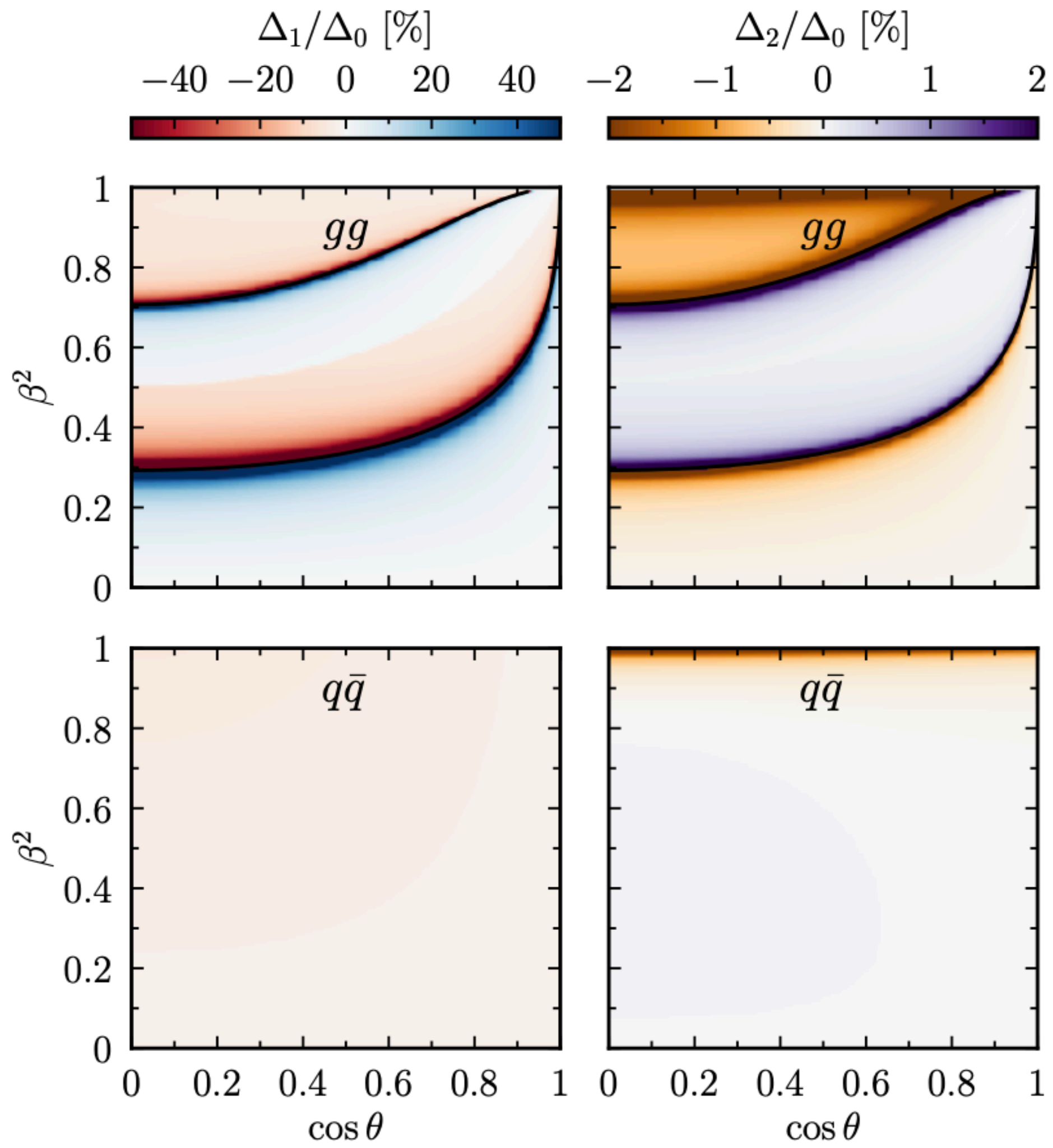
$$\Delta_2 \equiv \Delta - \Delta_1 - \Delta_0$$



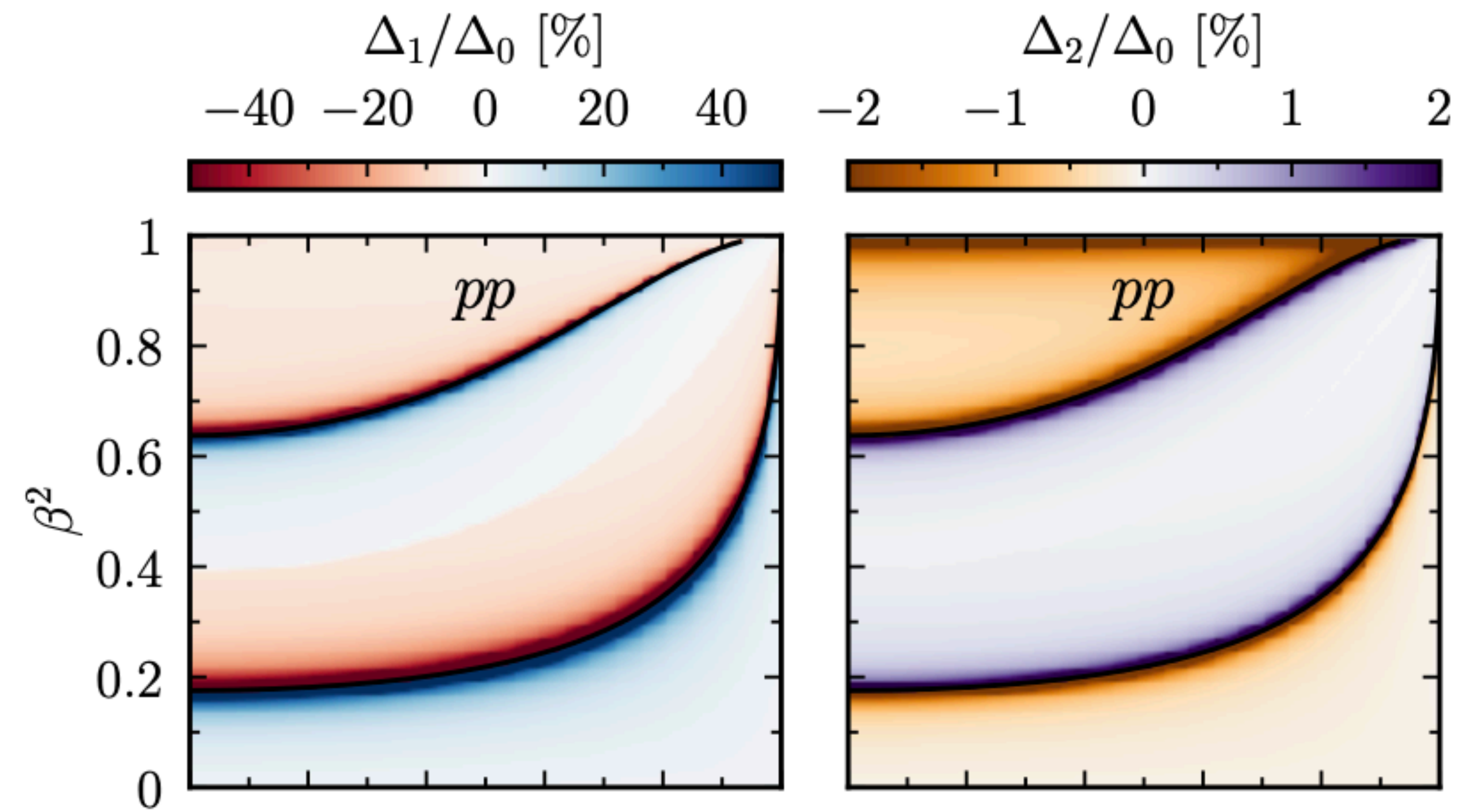
calculated with SMEFT R's up to $\mathcal{O}(\Lambda^{-4})$

SMEFT entanglement marker

separate channels



mixed state



SMEFT averaged concurrence

Average over the solid angle

$$\bar{R} = (4\pi)^{-1} \int d\Omega R(\hat{s}, \mathbf{k}), \quad \longrightarrow$$

PHC implies

$$\delta \equiv -C_z + |2C_{\perp}| - 1 > 0$$

$$C[\rho] = \max(\delta/2, 0)$$

(fixed beam basis)

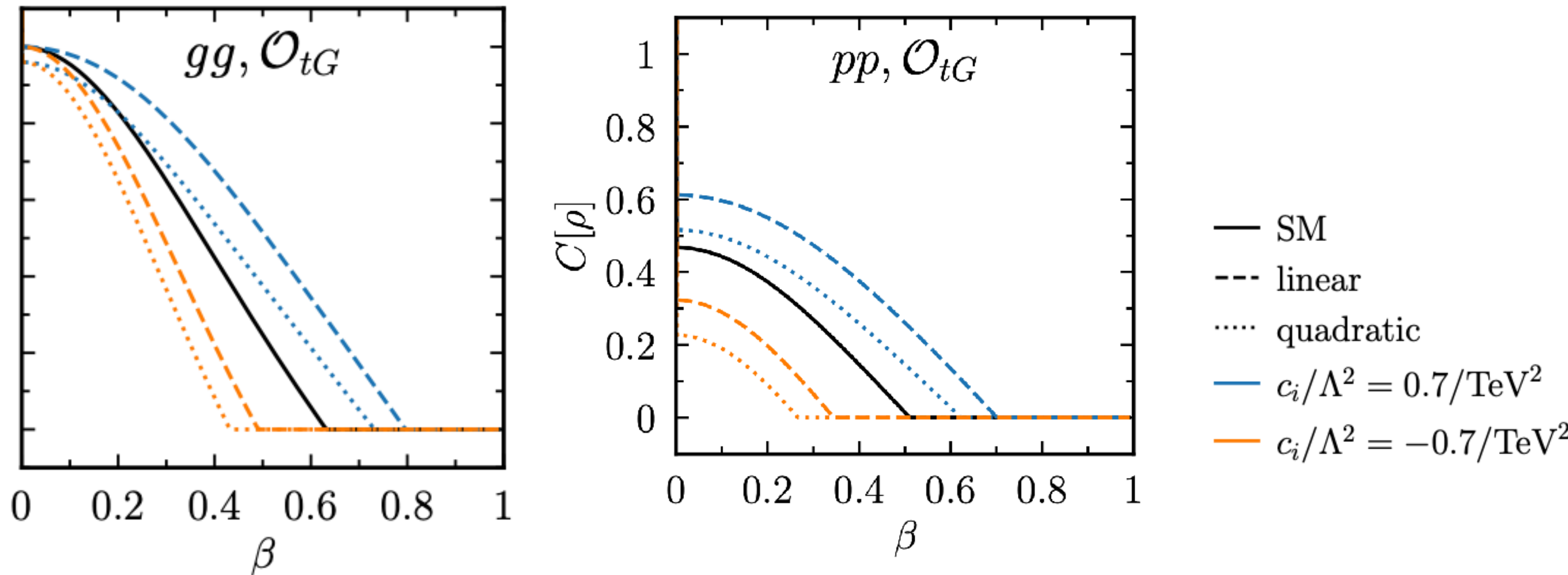
SMEFT averaged concurrence

Average over the solid angle

$$\bar{R} = (4\pi)^{-1} \int d\Omega R(\hat{s}, \mathbf{k}), \quad \longrightarrow \quad \delta \equiv -C_z + |2C_{\perp}| - 1 > 0$$

$$C[\rho] = \max(\delta/2, 0)$$

(fixed beam basis)



Tomography and reconstruction of the state

[Mahlon, Parke 10']
[Baumgart, Tweede 12']
[Afik and de Nova, 21']

$t \rightarrow W^+ + b$ ($W^+ \rightarrow \ell^+ + \nu$ or $\bar{d} + u$)

$$\frac{1}{\Gamma_t} \frac{d\Gamma}{d \cos \chi_i} = (1 + \alpha_i \cos \chi_i)/2$$

In the SM:

$$\alpha_i = \begin{cases} +1.0 & \ell^+ \text{ or } \bar{d}\text{-quark} \\ -0.31 & \bar{\nu} \text{ or } u\text{-quark} \\ -0.41 & b\text{-quark} \end{cases}$$

Tomography and reconstruction of the state

[Mahlon, Parke 10']

[Baumgart, Tweede 12']

[Afik and de Nova, 21']

$$t \rightarrow W^+ + b \quad (W^+ \rightarrow \ell^+ + \nu \text{ or } \bar{d} + u)$$

$$\frac{1}{\Gamma_t} \frac{d\Gamma}{d \cos \chi_i} = (1 + \alpha_i \cos \chi_i)/2$$

In the SMEFT:

[Zhang, Willenbrock, 11']

$$\begin{aligned}\alpha_b &= -\frac{m_t^2 - 2m_W^2}{m_t^2 + 2m_W^2} + \frac{\text{Re}C_{tW}v^2}{\Lambda^2 V_{tb}} \frac{8\sqrt{2}m_t m_W(m_t^2 - m_W^2)}{(m_t^2 + 2m_W^2)^2} \\ \alpha_v &= \frac{m_t^6 - 12m_t^4 m_W^2 + 3m_t^2 m_W^4 (3 + 8 \ln(m_t/m_W)) + 2m_W^6}{m_t^6 - 3m_t^2 m_W^4 + 2m_W^6} \\ &\quad - \frac{\text{Re}C_{tW}v^2}{\Lambda^2 V_{tb}} \frac{12\sqrt{2}m_t m_W(m_t^6 - 6m_t^4 m_W^2 + 3m_t^2 m_W^4 (1 + 4 \ln(m_t/m_W)) + 2m_W^6)}{(m_t^2 + 2m_W^2)^2 (m_t^2 - m_W^2)^2} \\ \alpha_{e^+} &= 1\end{aligned}$$

$\alpha_{\ell^+} = +1$ unchanged by dim-6 linear effects

In the SM:

$$\alpha_i = \begin{cases} +1.0 & \ell^+ \text{ or } \bar{d}-\text{quark} \\ -0.31 & \bar{\nu} \text{ or } u-\text{quark} \\ -0.41 & b-\text{quark} \end{cases}$$

* can be changed to dim-6 squared but very small

Diboson entanglement

Diboson entanglement

Massive spin-1 bosons (W,Z) have three polarisations  Qutrits!

Single vector boson

$$\rho = \frac{1}{3} \mathbb{I} + \sum_{i=1}^8 a_i \lambda_i \quad a_i : 8 \text{ real parameters}$$

Two vector bosons

$$\rho = \frac{1}{9} \mathbb{I} \otimes \mathbb{I} + \frac{1}{3} \sum_{i=1}^8 a_i \lambda_i \otimes \mathbb{I} + \frac{1}{3} \sum_{j=1}^8 b_j \mathbb{I} \otimes \lambda_j + \sum_{i=1}^8 \sum_{j=1}^8 c_{ij} \lambda_i \otimes \lambda_j$$

a_i, b_j, c_{ij} 8+8+64 real parameters

λ_i are Gell-Mann matrices

Concurrence for qutrits

[Horodecki, Horodecki, Horodecki, Horodecki, 09']

[Ashby-Pickering, Barr, Wierzchuca, '22]

How is the concurrence for qutrits? Not as simple as in the qubit case

$$C(\rho) = \inf \left[\sum_i p_i c(|\psi_i\rangle) \right]$$

$$c(|\psi_i\rangle) = \sqrt{2(1 - \text{tr}_A[(\text{tr}_B |\psi_i\rangle\langle\psi_i|)^2])}$$

Infimum of all ensembles of the decomposition $\rho = \sum_i p_i |\psi_i\rangle\langle\psi_i|$

... complicated optimisation problem

$$0 \leq C(\rho) \leq \frac{2}{\sqrt{3}}$$
$$C(\rho) > 0 \longrightarrow \text{entangled}$$

Only calculable for pure states.

Concurrence Bounds for qutrits

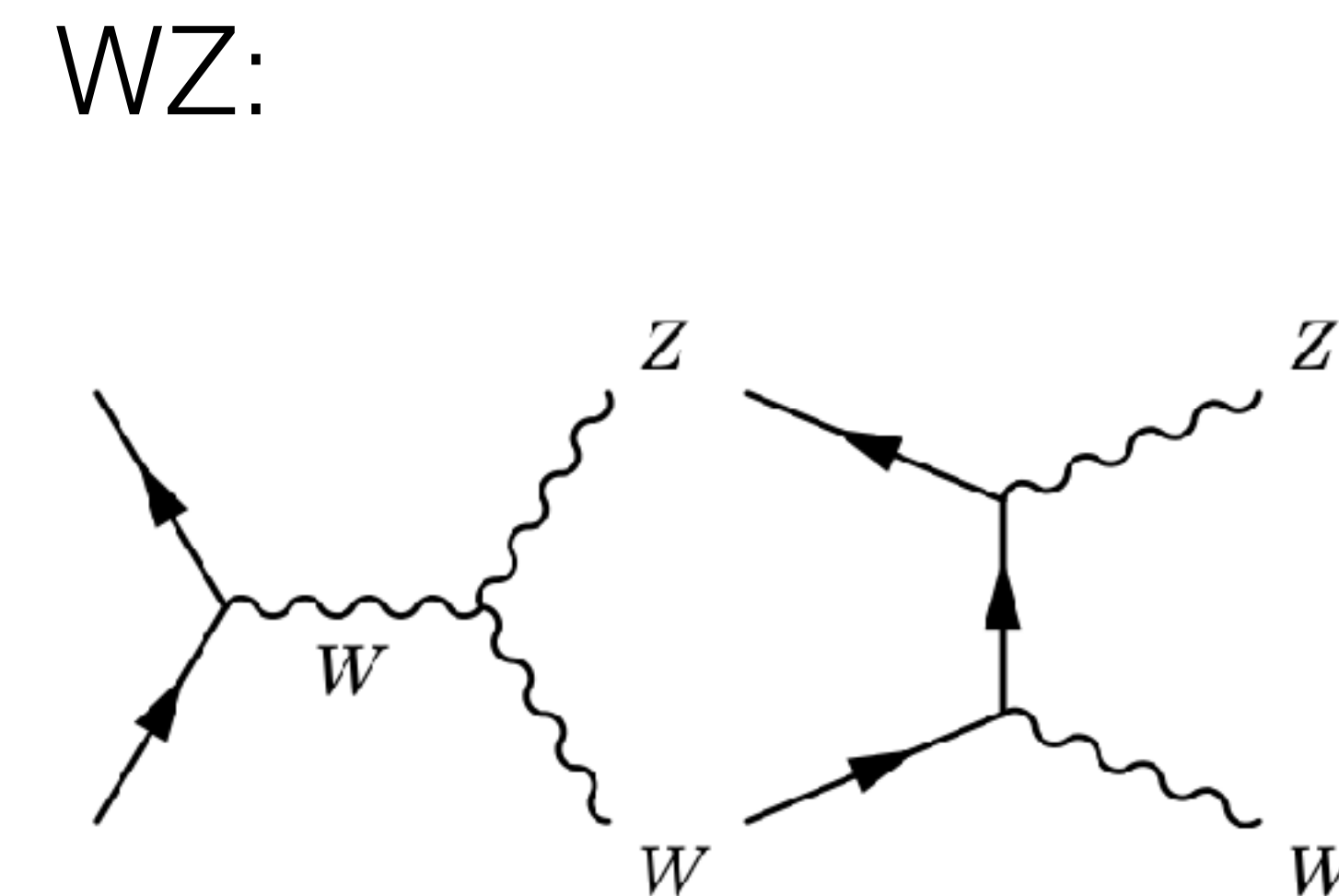
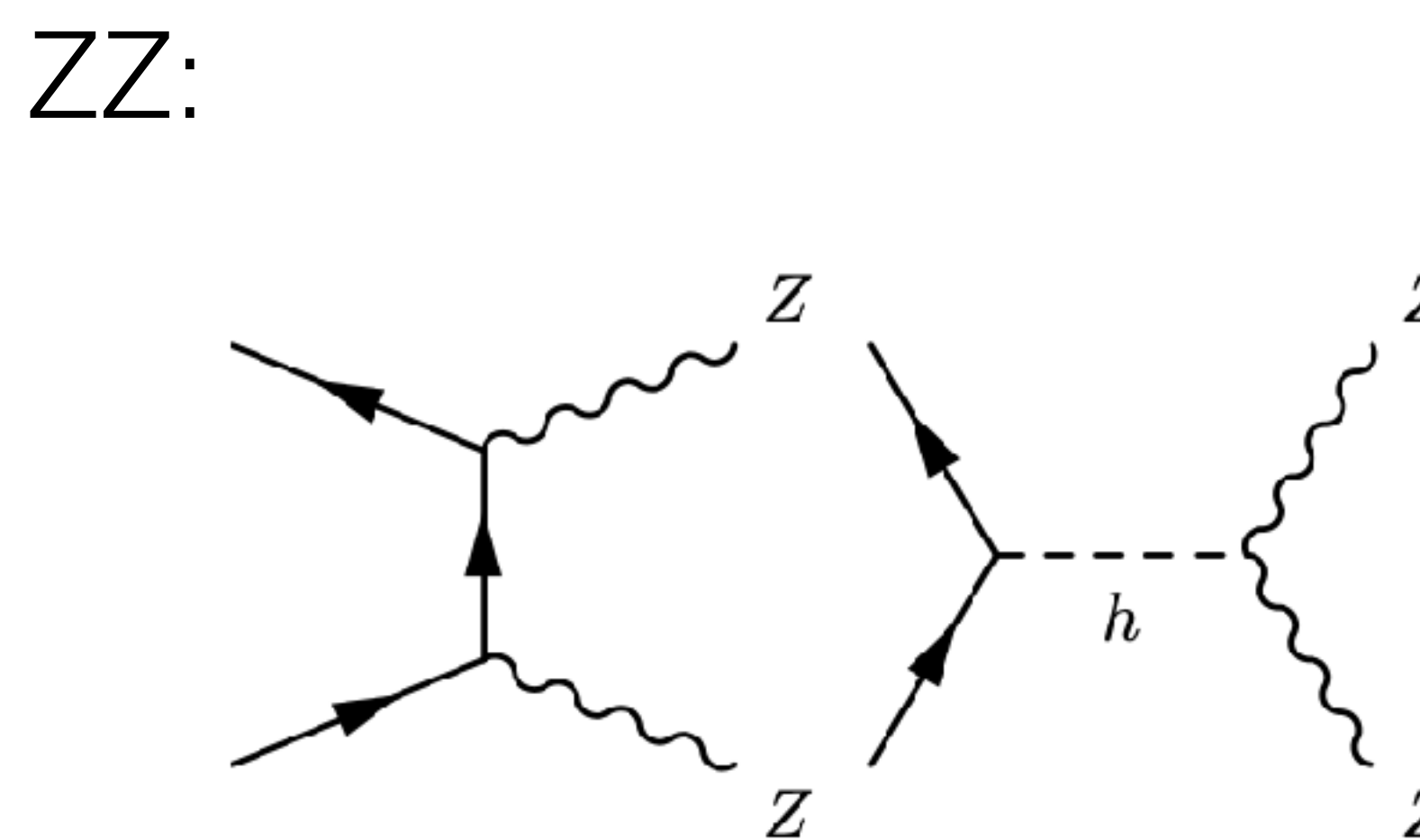
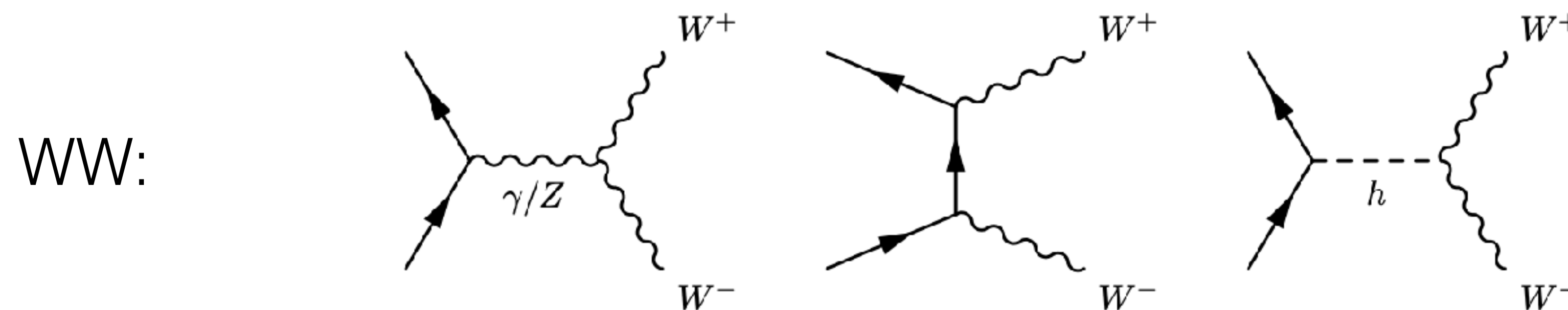
However, we can define lower and upper bounds $\mathcal{C}_{\text{LB}} \leq \mathcal{C}(\rho) \leq \mathcal{C}_{\text{UB}}$,

Lower: $(\mathcal{C}(\rho))^2 \geq 2 \max(0, \text{Tr}[\rho^2] - \text{Tr}[\rho_A^2], \text{Tr}[\rho^2] - \text{Tr}[\rho_B^2]) \equiv \mathcal{C}_{\text{LB}}^2,$

Upper: $(\mathcal{C}(\rho))^2 \leq 2 \min(1 - \text{Tr}[\rho_A^2], 1 - \text{Tr}[\rho_B^2]) \equiv \mathcal{C}_{\text{UB}}^2,$

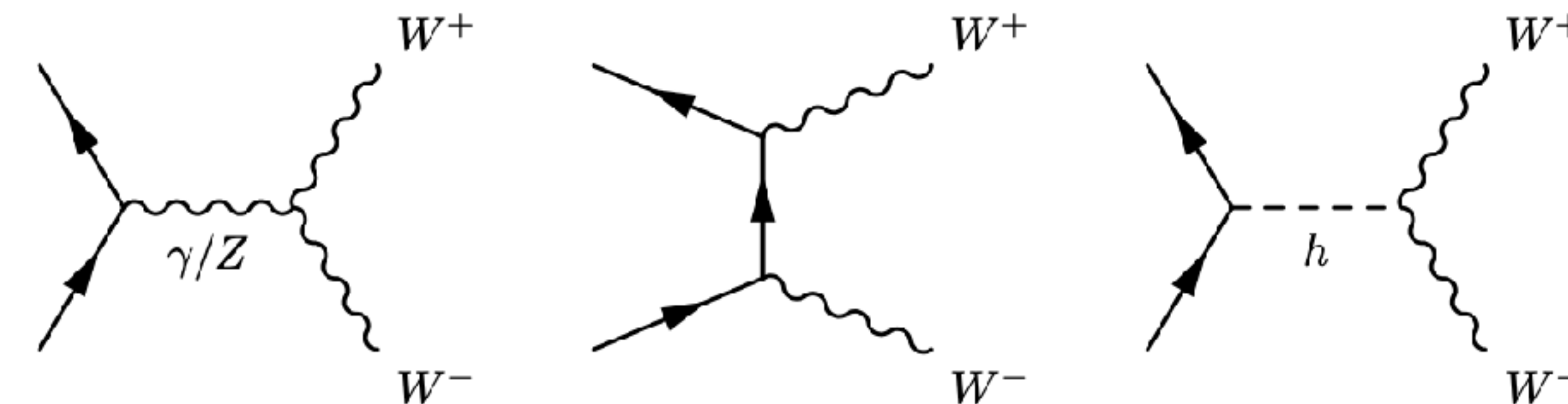
For a pure state: $P(\rho) = \text{tr}\rho^2 = 1 \quad \longrightarrow \quad \mathcal{C}_{\text{LB}}(\rho) = \mathcal{C}(\rho) = \mathcal{C}_{\text{UB}}(\rho)$

EW boson production at colliders

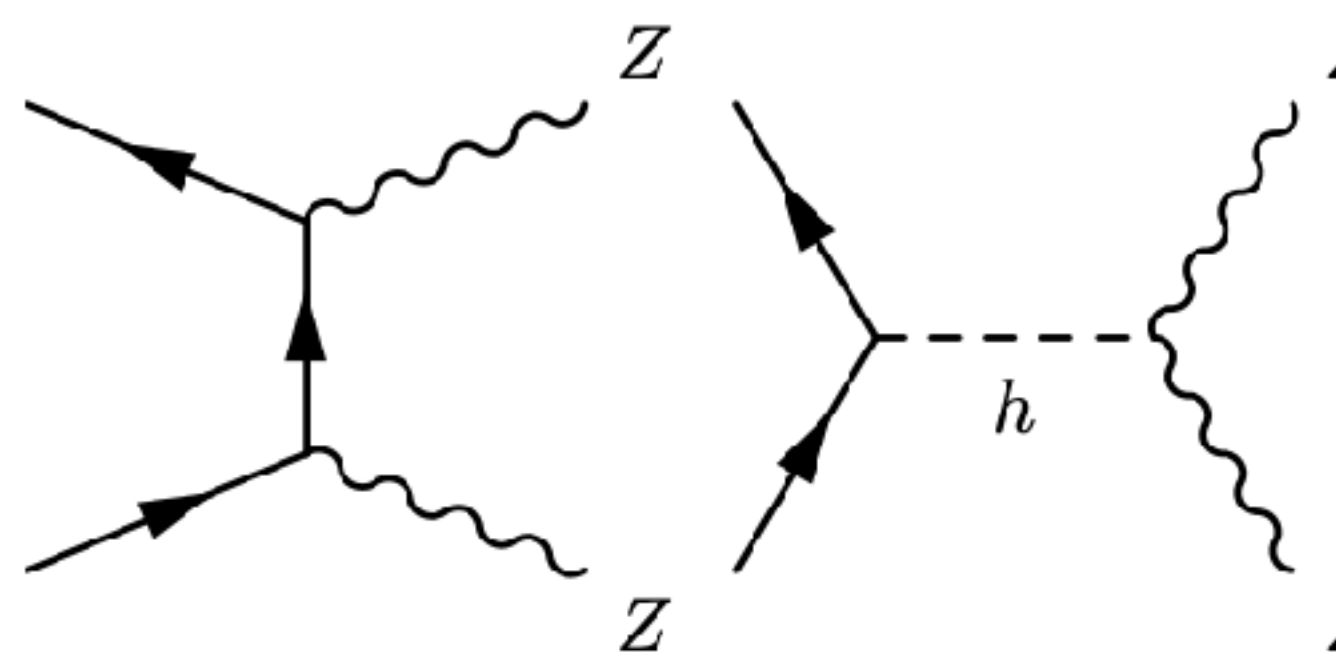


EW boson production at colliders

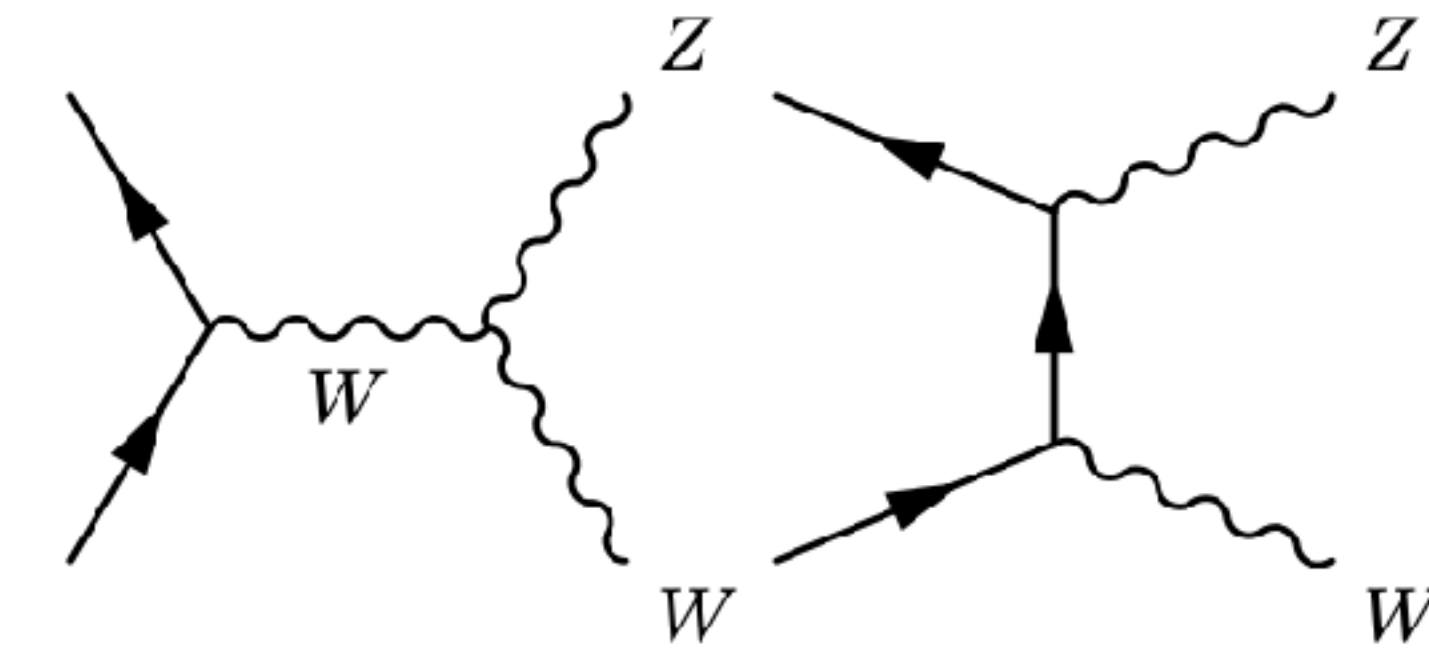
WW:



ZZ:



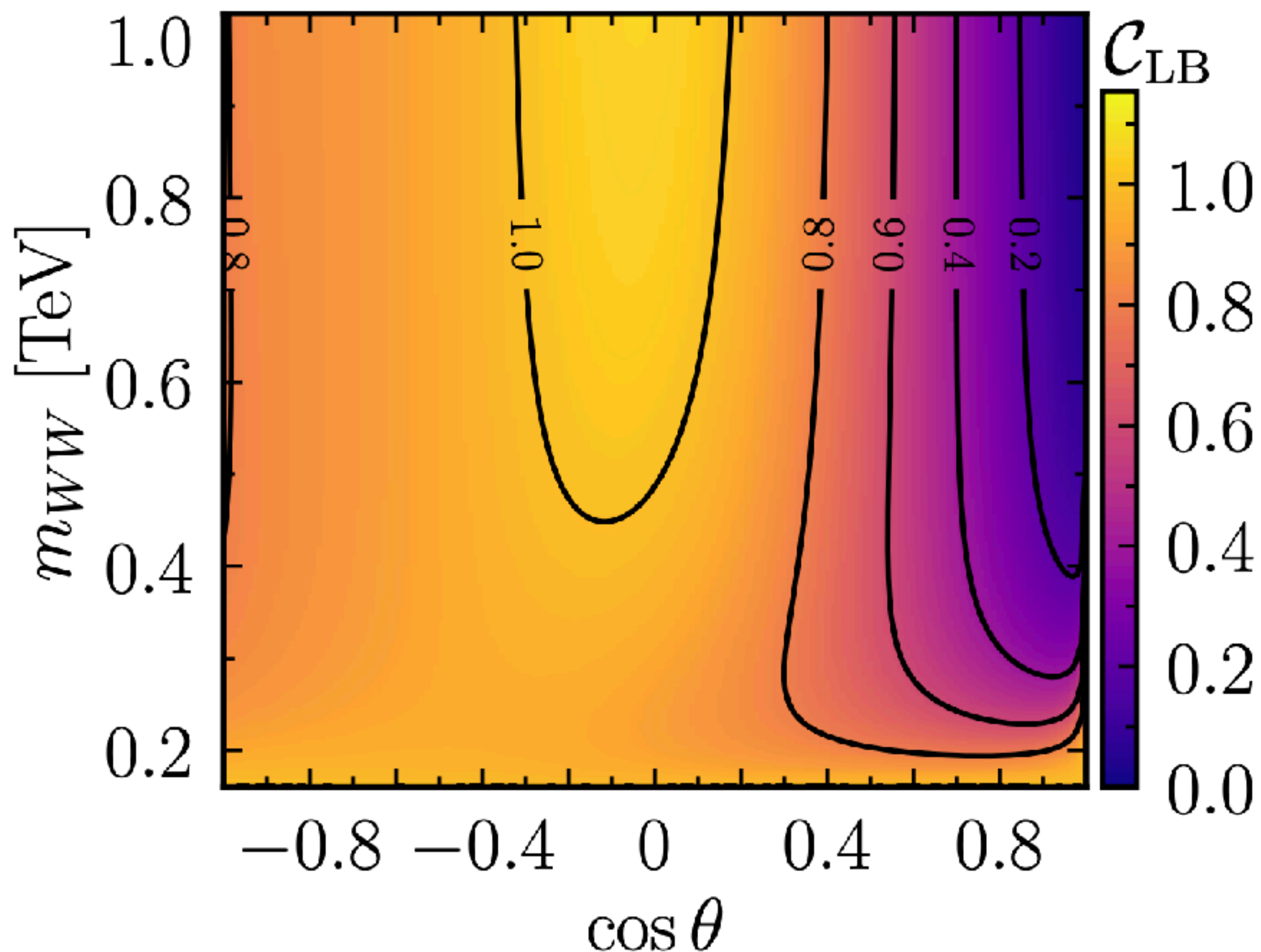
WZ:



What's the story for the Standard Model?

$$e^+ e^- \rightarrow W^+ W^-$$

Lower bound:



No symmetry around $\theta = \pi/2$ as in ttbar

Entanglement is mostly present across the phase space

Zero entanglement at $\theta = 0$

High entanglement at central HE region

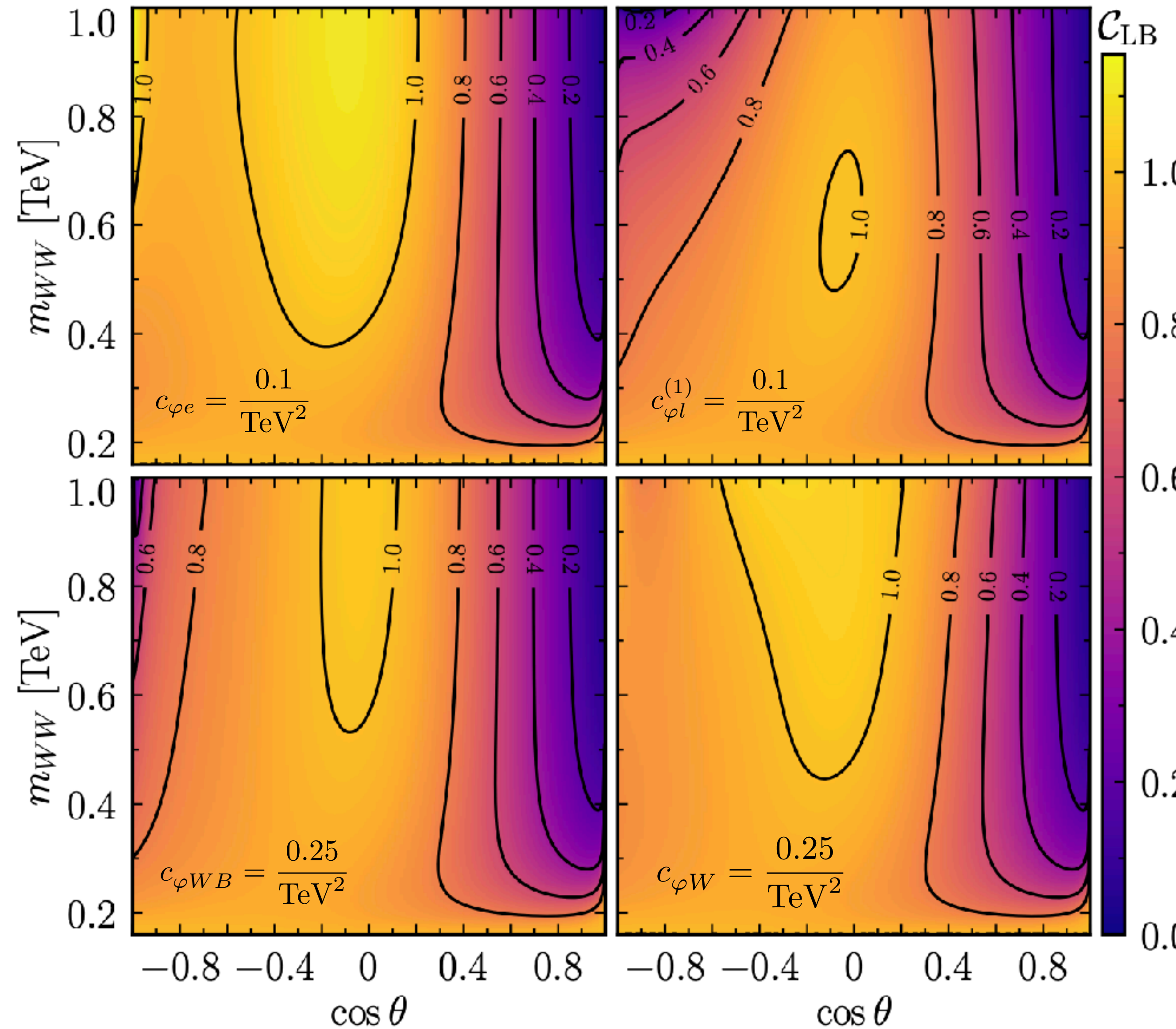
Relevant SMEFT Operators for diboson

Operator	Coefficient	Definition	95 % CL bounds	bosonic operators			
two-fermion operators							
$\mathcal{O}_{\varphi u}$	$c_{\varphi u}$	$i(\varphi^\dagger \overset{\leftrightarrow}{D}_\mu \varphi)(\bar{u} \gamma^\mu u)$	$[-0.17, 0.14]$	\mathcal{O}_W	c_W	$\varepsilon_{IJK} W_{\mu\nu}^I W^{J,\nu\rho} W_\rho^{K,\mu},$	$[-0.18, 0.22]$
$\mathcal{O}_{\varphi d}$	$c_{\varphi d}$	$i(\varphi^\dagger \overset{\leftrightarrow}{D}_\mu \varphi)(\bar{d} \gamma^\mu d)$	$[-0.07, 0.09]$	$\mathcal{O}_{\varphi W}$	$c_{\varphi W}$	$\left(\varphi^\dagger \varphi - \frac{v^2}{2}\right) W_I^{\mu\nu} W_{\mu\nu}^I$	$[-0.15, 0.30]$
$\mathcal{O}_{\varphi q}^{(1)}$	$c_{\varphi q}^{(1)}$	$i(\varphi^\dagger \overset{\leftrightarrow}{D}_\mu \varphi)(\bar{q} \gamma^\mu q)$	$[-0.06, 0.22]$	$\mathcal{O}_{\varphi B}$	$c_{\varphi B}$	$\left(\varphi^\dagger \varphi - \frac{v^2}{2}\right) B_{\mu\nu} B^{\mu\nu}$	$[-0.11, 0.11]$
$\mathcal{O}_{\varphi q}^{(3)}$	$c_{\varphi q}^{(3)}$	$i(\varphi^\dagger \overset{\leftrightarrow}{D}_\mu \tau_I \varphi)(\bar{q} \gamma^\mu \tau^I q)$	$[-0.21, 0.05]$	$\mathcal{O}_{\varphi WB}$	$c_{\varphi WB}$	$(\varphi^\dagger \tau_I \varphi) B^{\mu\nu} W_{\mu\nu}^I$	$[-0.17, 0.27]$
$\mathcal{O}_{\varphi e}$	$c_{\varphi e}$	$i(\varphi^\dagger \overset{\leftrightarrow}{D}_\mu \varphi)(\bar{e} \gamma^\mu e)$	$[-0.21, 0.26]$	$\mathcal{O}_{\varphi D}$	$c_{\varphi D}$	$(\varphi^\dagger D^\mu \varphi)^\dagger (\varphi^\dagger D_\mu \varphi)$	$[-0.52, 0.43]$
four-fermion operator							
$\mathcal{O}_{\varphi l}^{(1)}$	$c_{\varphi l}^{(1)}$	$i(\varphi^\dagger \overset{\leftrightarrow}{D}_\mu \varphi)(\bar{l} \gamma^\mu l)$	$[-0.11, 0.13]$	\mathcal{O}_{ll}	c_{ll}	$(\bar{l} \gamma_\mu l)(\bar{l} \gamma^\mu l)$	$[-0.16, 0.02]$
$\mathcal{O}_{\varphi l}^{(3)}$	$c_{\varphi l}^{(3)}$	$i(\varphi^\dagger \overset{\leftrightarrow}{D}_\mu \tau_I \varphi)(\bar{l} \gamma^\mu \tau^I l)$	$[-0.21, 0.05]$				

Bounds from [SMEFit Collaboration '21]

SMEFT entanglement deviations

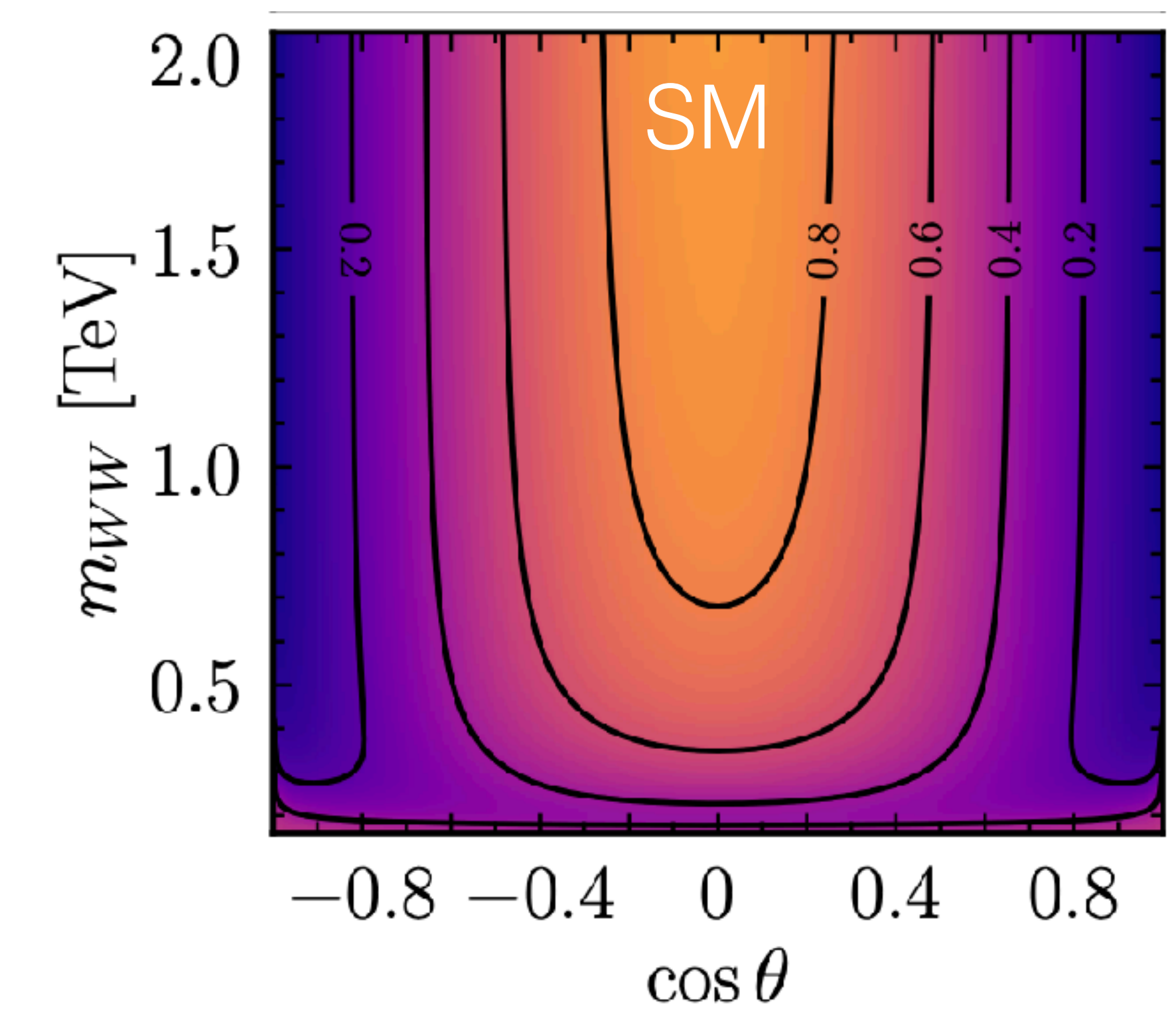
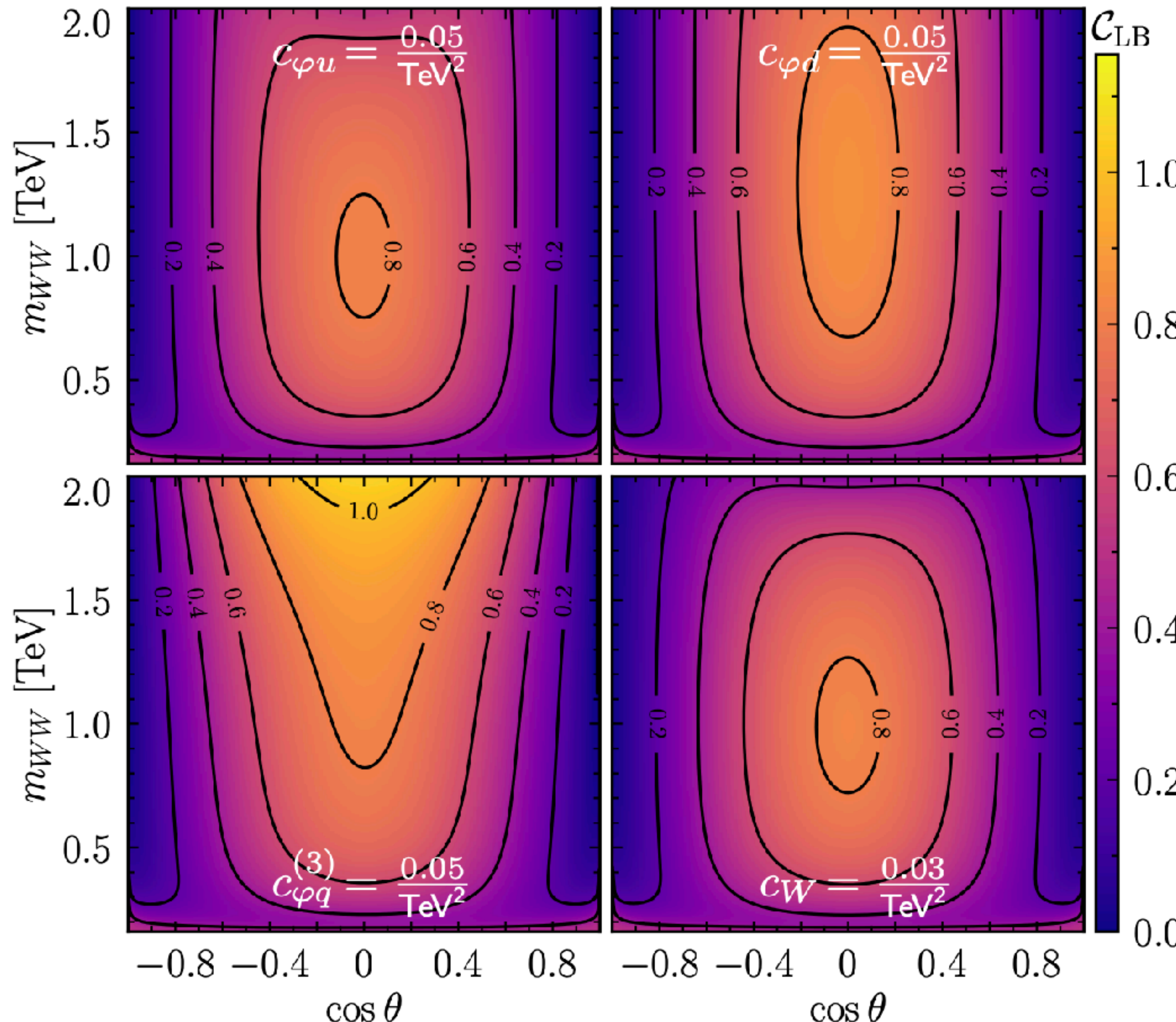
$e^+e^- \rightarrow W^+W^-$



- $\mathcal{O}_{\varphi e}$ changes $Ze_R^+e_R^-$ vertex
 - more ent. in central and backward HE
- $\mathcal{O}_{\varphi l}^{(1)}$ changes $Ze_L^+e_L^-$ vertex
 - less ent. in central and backward HE
- $\mathcal{O}_{\varphi WB}$ changes TGC coupling
- \mathcal{O}_W new Lorentz structure
 - small effect

SMEFT entanglement deviations

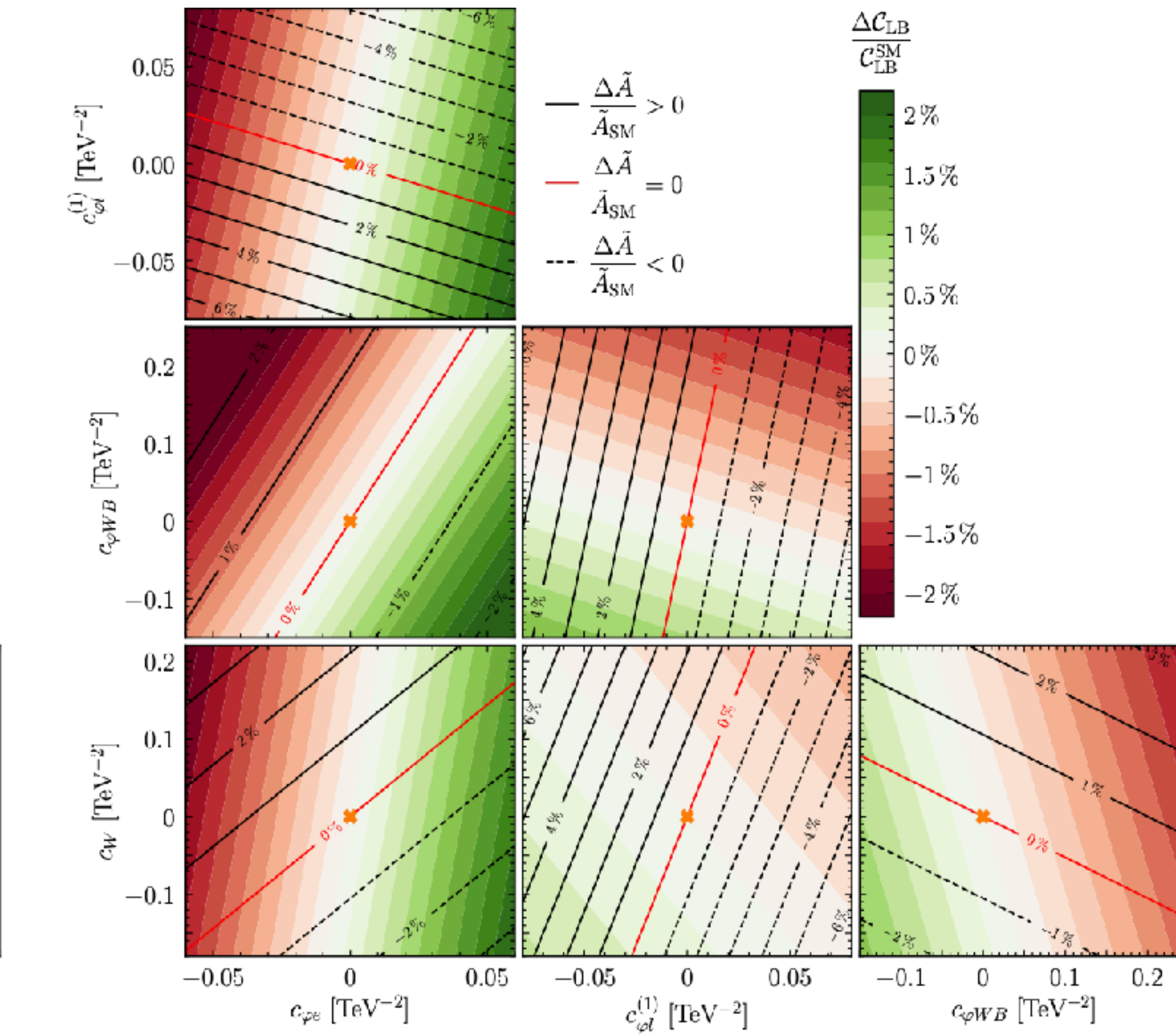
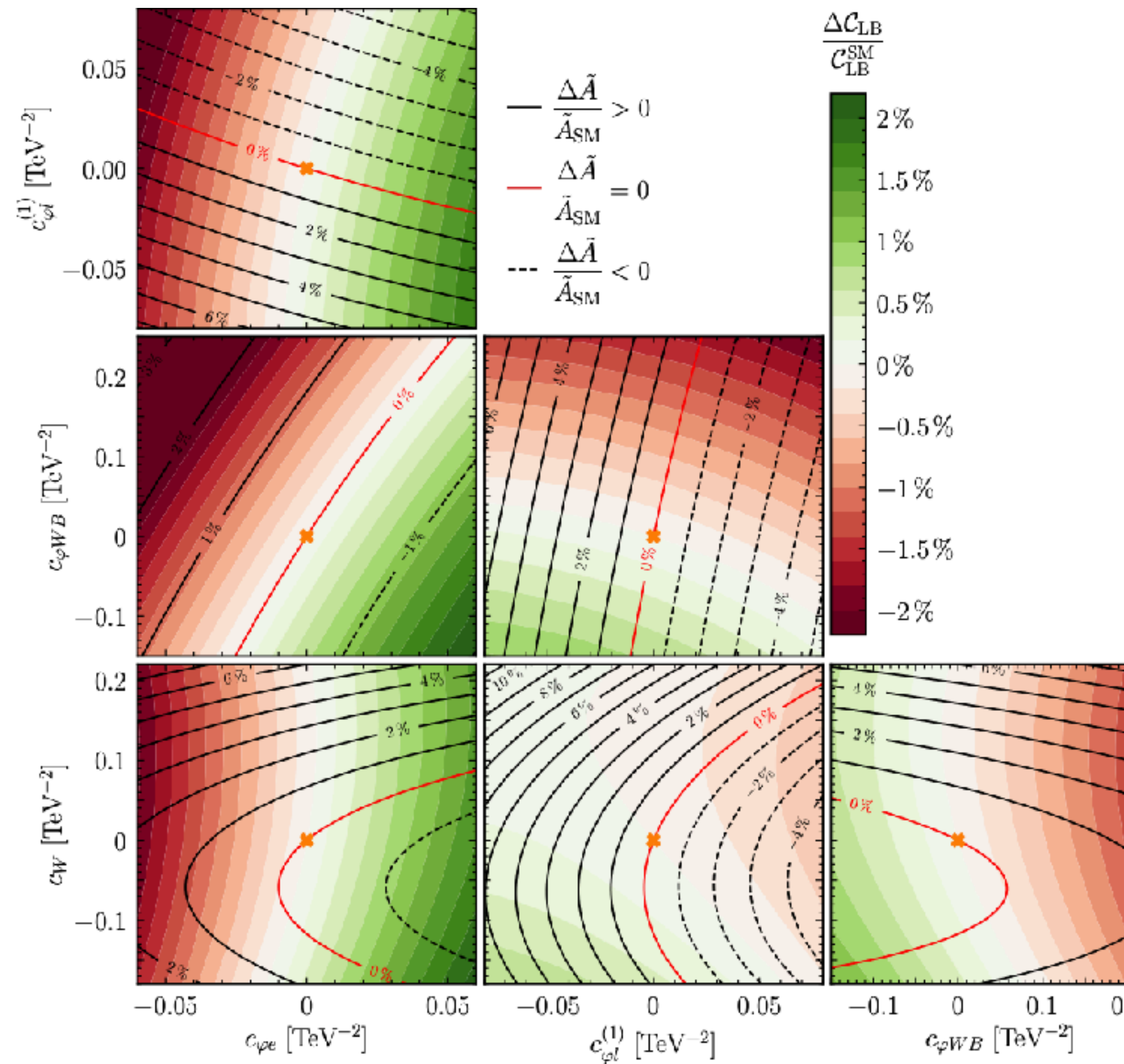
$pp \rightarrow W^+W^-$



Similar balance changes
for hadron collider.

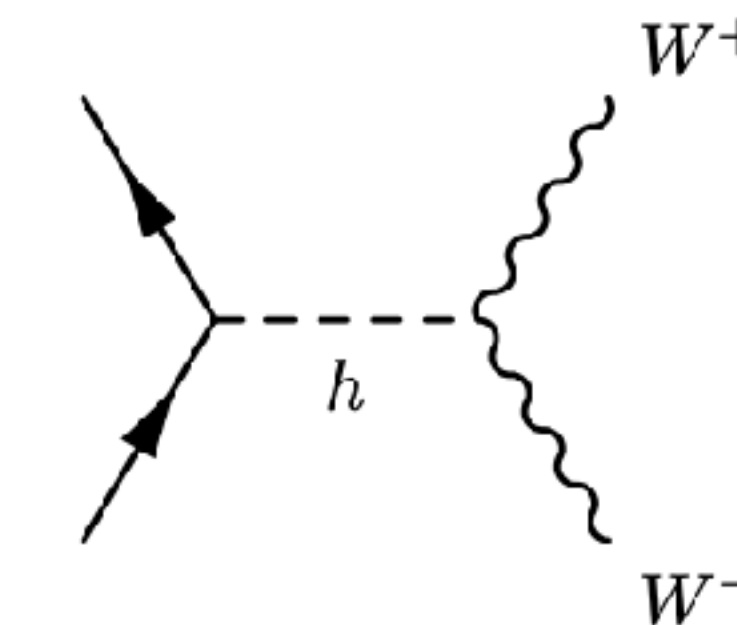
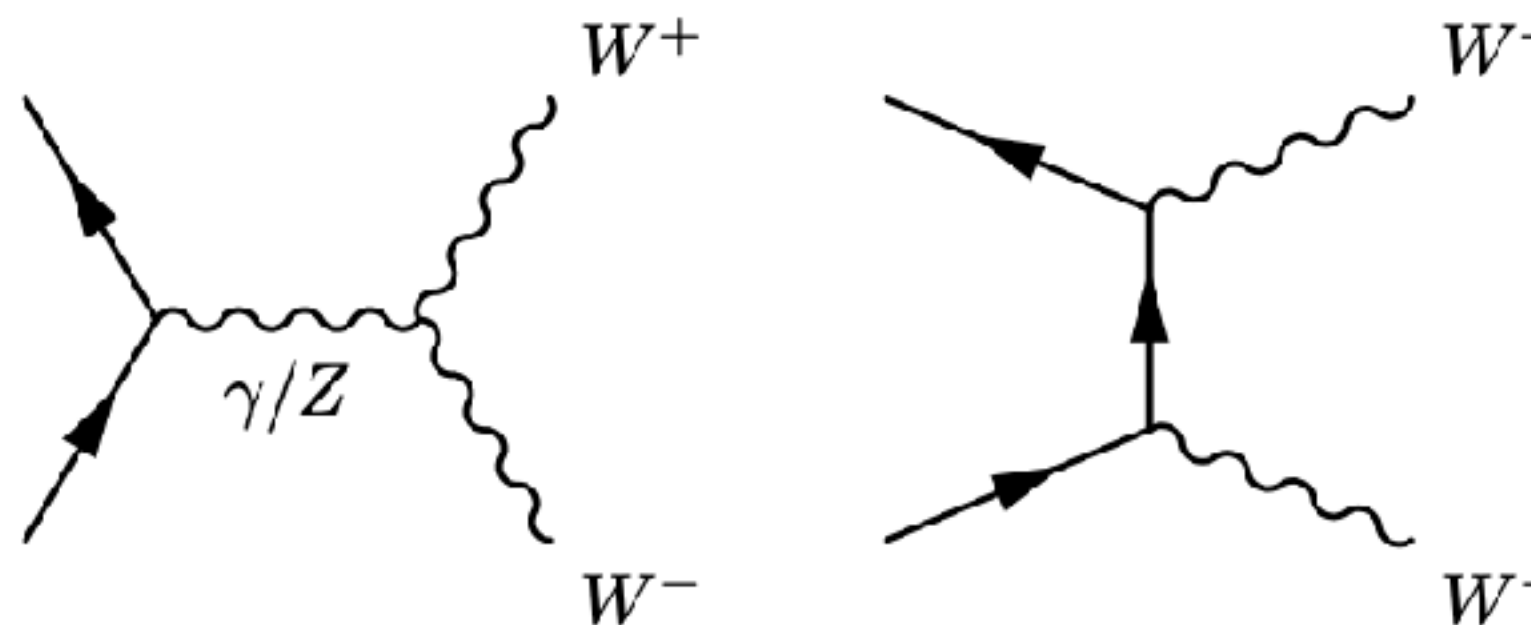
SMEFT entanglement deviations: Central region

$$m_{WW} = 500 \text{ GeV} \quad \cos \theta = 0$$

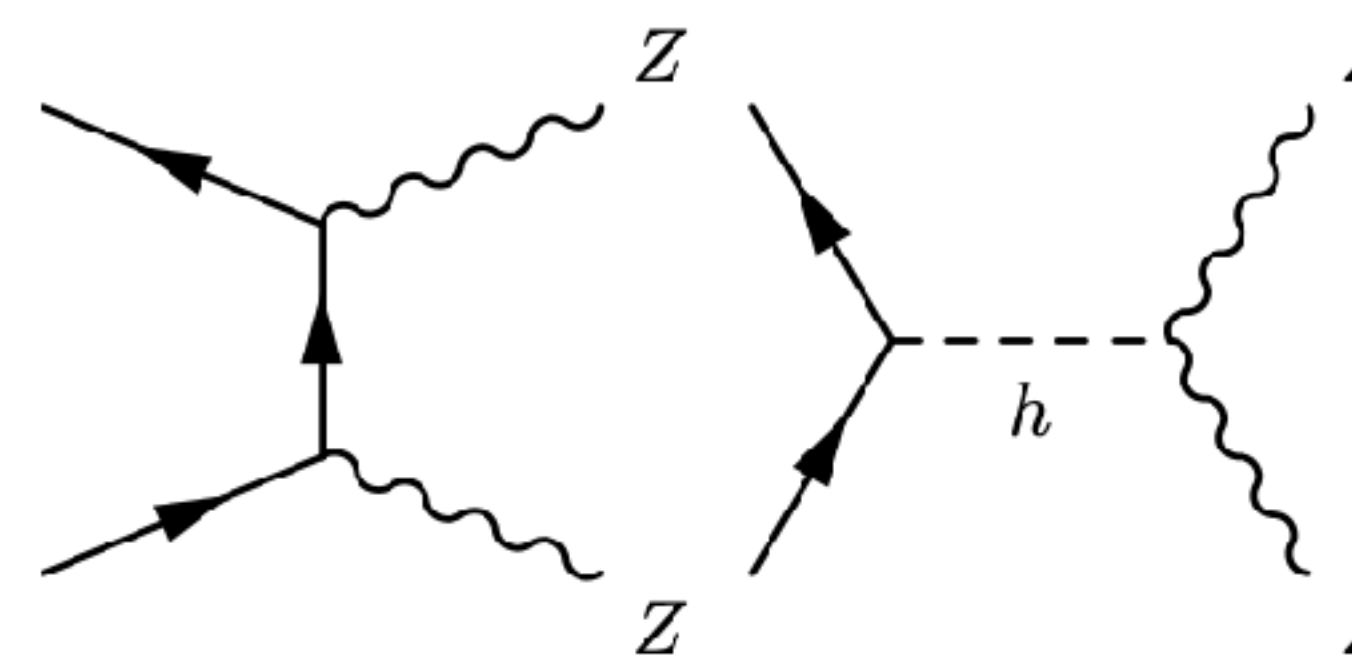


EW boson production at colliders

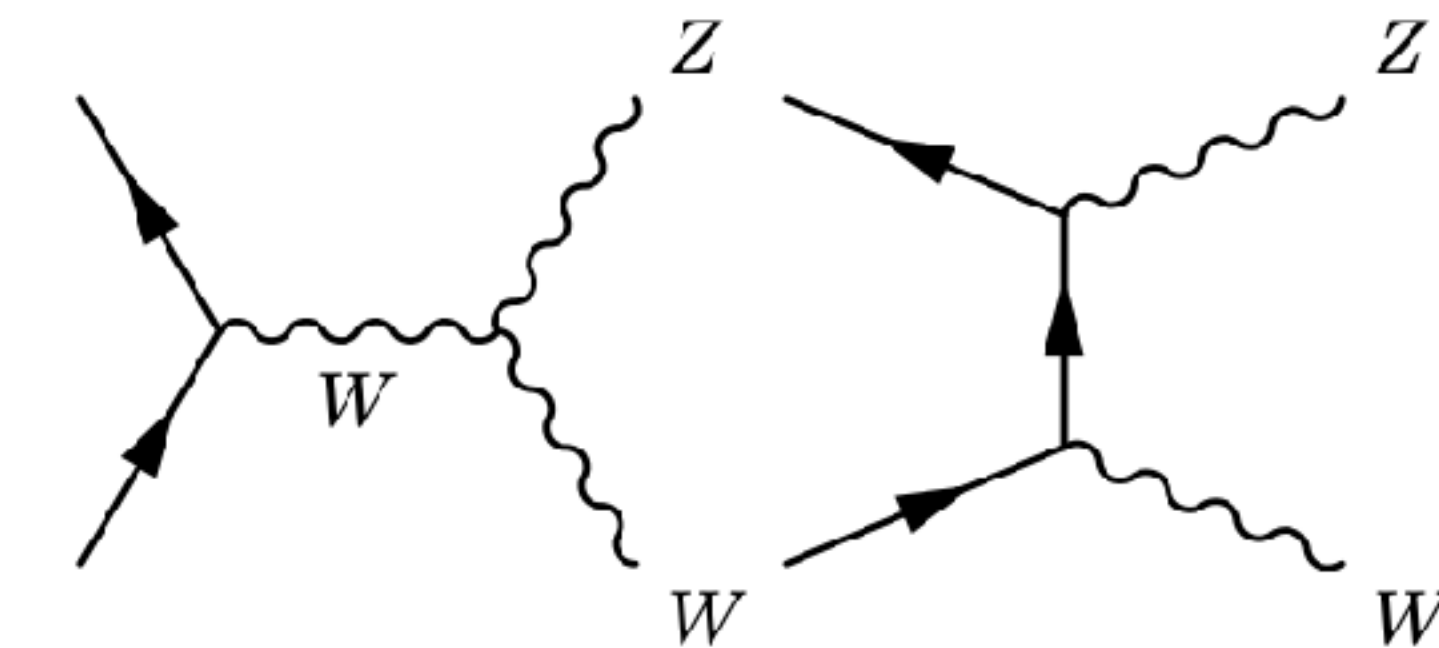
W.W.



zz.

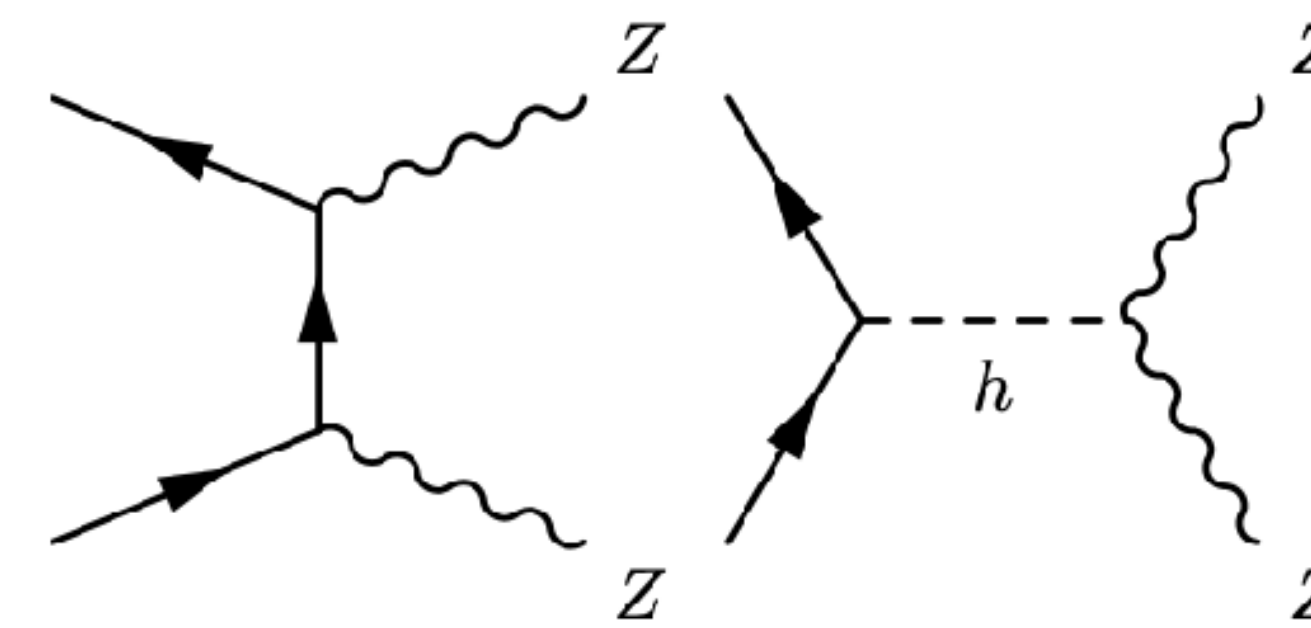
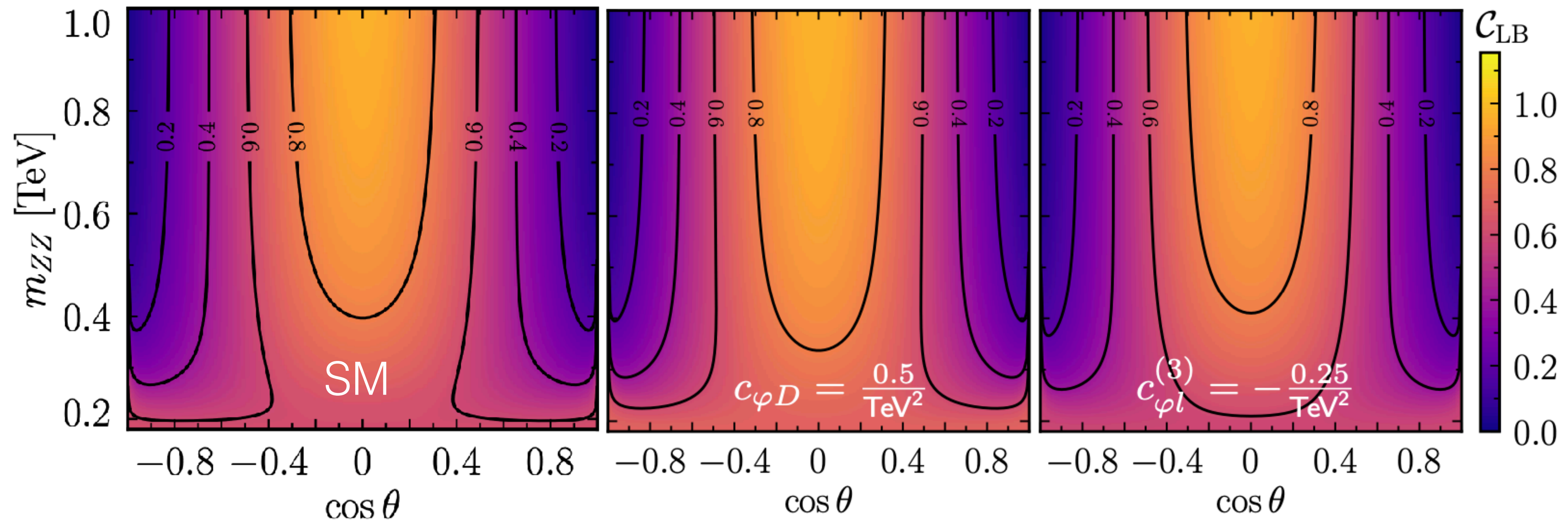


WZ



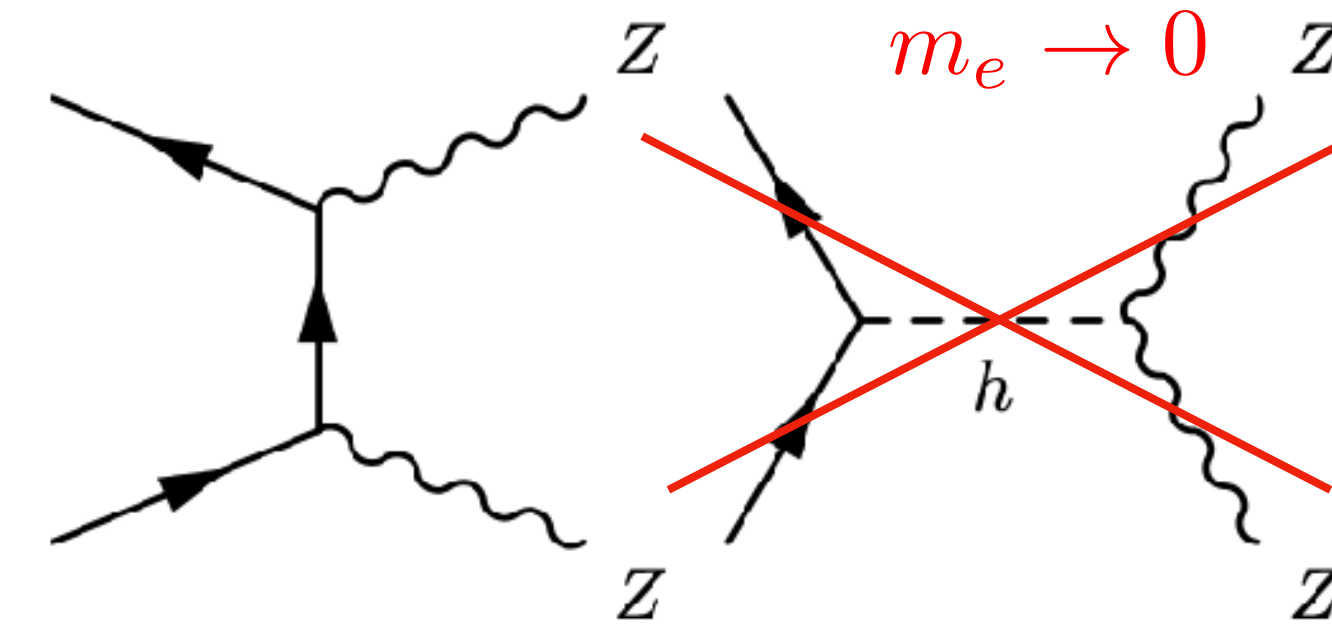
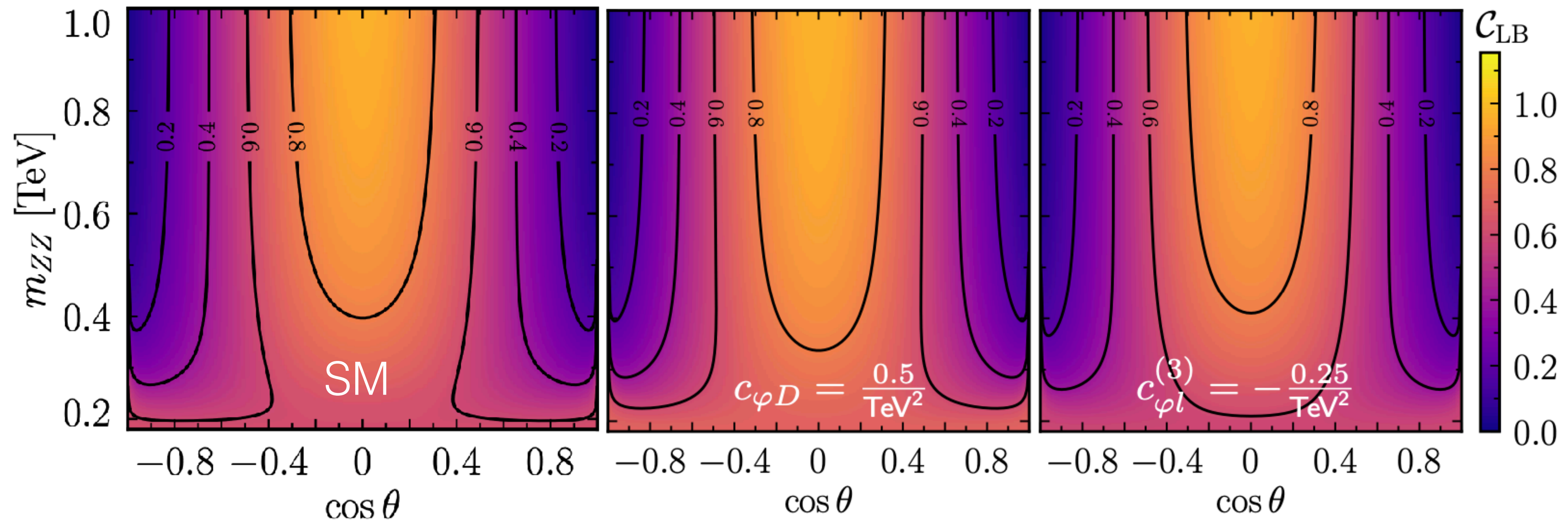
EW boson production at colliders

$e^+e^- \rightarrow ZZ$



EW boson production at colliders

$e^+e^- \rightarrow ZZ$



SMEFT just change the balance
between RH and LH couplings

effects are reduced in $pp \rightarrow ZZ$

Perturbative Unitarity and Entanglement

The density matrix (and angular observables) are sensitive to new directions

$$e^+ e^- \rightarrow W^+ W^-$$

$(\lambda_1 \lambda_2 \alpha \beta)$	SM	EFT $\Lambda^{-2} : c_{WWW}$
+ - 00	$-2\sqrt{2}G_F m_Z^2 \sin \theta$	-
+ - - +	$2\sqrt{2}G_F m_W^2 \sin \theta$	-
+ - +-	$-\frac{1}{\sqrt{2}}G_F m_W^2 \sin^3 \theta \csc^4(\theta/2)$	-
+ - ±±	-	$3 \cdot 2^{1/4} \sqrt{G_F} m_W \sin \theta (4m_W^2 x^2 - m_Z^2)$
+ - 0±	-	$-3 \cdot 2^{3/4} \sqrt{G_F} m_W^3 (\pm 1 + \cos \theta) x$
+ - ±0	-	$-3 \cdot 2^{3/4} \sqrt{G_F} m_W^3 (\mp 1 + \cos \theta) x$
<hr/>		
- + 00	$2\sqrt{2}G_F(m_Z^2 - m_W^2) \sin \theta$	-
- + ±±	-	$6 \cdot 2^{1/4} \sqrt{G_F} m_W(m_Z^2 - m_W^2) \sin \theta$

Perturbative Unitarity and Entanglement

The density matrix (and angular observables) are sensitive to new directions

$$e^+ e^- \rightarrow W^+ W^-$$

$(\lambda_1 \lambda_2 \alpha \beta)$	SM	EFT $\Lambda^{-2} : c_{WWW}$
+ - 00	$-2\sqrt{2}G_F m_Z^2 \sin \theta$	 -
+ - - +	$2\sqrt{2}G_F m_W^2 \sin \theta$	 -
+ - +-	$-\frac{1}{\sqrt{2}}G_F m_W^2 \sin^3 \theta \csc^4(\theta/2)$	 -
+ - ±±	-  $3 \cdot 2^{1/4} \sqrt{G_F} m_W \sin \theta (4m_W^2 x^2 - m_Z^2)$	
+ - 0±	-  $-3 \cdot 2^{3/4} \sqrt{G_F} m_W^3 (\pm 1 + \cos \theta) x$	
+ - ±0	-  $-3 \cdot 2^{3/4} \sqrt{G_F} m_W^3 (\mp 1 + \cos \theta) x$	
<hr/>		
- + 00	$2\sqrt{2}G_F(m_Z^2 - m_W^2) \sin \theta$	 -
- + ±±	-  $6 \cdot 2^{1/4} \sqrt{G_F} m_W(m_Z^2 - m_W^2) \sin \theta$	
<hr/>		

No interference!



Cross-section

$$\tilde{A}(\mathcal{O}_W) \sim 0$$

Perturbative Unitarity and Entanglement

$(\lambda_1 \lambda_2 \alpha \beta)$	SM	EFT $\Lambda^{-2} : c_{WWW}$
+ - 00	$-2\sqrt{2}G_F m_Z^2 \sin \theta$	-
+ - - +	$2\sqrt{2}G_F m_W^2 \sin \theta$	-
+ - +-	$-\frac{1}{\sqrt{2}}G_F m_W^2 \sin^3 \theta \csc^4(\theta/2)$	-
+ - ±±	-	$3 \cdot 2^{1/4} \sqrt{G_F} m_W \sin \theta (4m_W^2 x^2 - m_Z^2)$
+ - 0±	-	$-3 \cdot 2^{3/4} \sqrt{G_F} m_W^3 (\pm 1 + \cos \theta) x$
+ - ±0	-	$-3 \cdot 2^{3/4} \sqrt{G_F} m_W^3 (\mp 1 + \cos \theta) x$
- + 00	$2\sqrt{2}G_F(m_Z^2 - m_W^2) \sin \theta$	-
- + ±±	-	$6 \cdot 2^{1/4} \sqrt{G_F} m_W(m_Z^2 - m_W^2) \sin \theta$

$$\rho = \begin{bmatrix} \mathcal{M}_{++} & \mathcal{M}_{++}^* & & \\ \mathcal{M}_{+-} & \mathcal{M}_{++}^* & \cdots & \\ \mathcal{M}_{+-}^* & \mathcal{M}_{+-} & \cdots & \\ \vdots & \ddots & & \end{bmatrix}$$

The spin-density matrix has different helicity products

$$\tilde{a}_1(\mathcal{O}_W) \simeq \tilde{b}_1(\mathcal{O}_W) \simeq \bar{c}_W 2^{5/4} x \cos^4(\theta/2)(\cos \theta + 3) \csc \theta,$$

Entanglement is sensitive to off-diagonal contractions

$$\tilde{c}_{13} \simeq 3 \bar{c}_W \cdot 2^{3/4} \cos^2(\theta/2)(3 \cos \theta + 1) \cot(\theta/2) x$$

Recovers the energy growth!

Conclusions

SM induces maximal entanglement points/regions in ttbar

Purely linear interference SMEFT effects vanish in these regions!

Quadratic interference decreases the entanglement at these points

Missing dim-8 linear interference and double-insertions at $\mathcal{O}(\Lambda^{-4})$

Conclusions

SM induces maximal entanglement points/regions in ttbar

Purely linear interference SMEFT effects vanish in these regions!

Quadratic interference decreases the entanglement at these points

Missing dim-8 linear interference and double-insertions at $\mathcal{O}(\Lambda^{-4})$

Diboson production: Qutrits

Entanglement measures are more subtle

$e^+e^- \rightarrow W^+W^-$, $pp \rightarrow W^+W^-$ and $pp \rightarrow WZ$ are sensitive to dim-6 modifications

while $e^+e^- \rightarrow ZZ$ and $pp \rightarrow ZZ$ are less (but potentially for dim-8)



THE UNIVERSITY
of EDINBURGH